This document was prepared for the ETI by third parties under contract to the ETI. The ETI is making these documents and data available to the public to inform the debate on low carbon energy innovation and deployment.

Programme Area: Marine

Project: PerAWAT

Title: GH Near Wake Modelling Report

Abstract:

This document outlines the issues associated with modelling a region of the wake behind a tidal turbine rotor, known as the near wake or the beginning of the far wake region. A review of the existing literature is presented which provides an overview of both the applicable modelling options and previous experimental campaigns which characterise the wake region of interest. The GH near wake model is described and the modelling approach justified. The model is used to predict the three dimensional flow field which is then passed to the GH far wake model as an input. The GH Blockage model feeds the model when appropriate, providing a corrected rotor thrust and an altered flow field around the turbine. A list of key assumptions that the GH near wake model makes is provided along with the relevant references to existing theory. The method by which the mathematical models are implemented into a working code is described, as is the way in which the GH near wake model is to be incorporated within the GH TidalFarmer Beta code. Flow diagrams of the GH near wake model algorithms are presented and example outputs provided.

Context:

The Performance Assessment of Wave and Tidal Array Systems (PerAWaT) project, launched in October 2009 with £8m of ETI investment. The project delivered validated, commercial software tools capable of significantly reducing the levels of uncertainty associated with predicting the energy yield of major wave and tidal stream energy arrays. It also produced information that will help reduce commercial risk of future large scale wave and tidal array developments.

ETI Marine Programme Project
PerAWaT MA1003
WG3WP4 D2 GH NEAR WAKE MODELLING REPORT

Client	**Energy Technologies Institute**
Contact	Geraldine Newton-Cross
Document No	104329/BR/02
Issue	2.0
Classification	Not to be disclosed other than in line with the terms of the Technology Contract
Date	15th June 2010

Author:

M D Thomson

Checked by:

J I Whelan

Approved by:

R I Rawlinson-Smith

DISCLAIMER

1. This report is intended for the use of the Client on whose instructions it has been prepared, and who has entered into a written agreement directly with Garrad Hassan & Partners Limited ("GH"). GH's liability to the Client is set out in that agreement. GH shall have no liability to third parties for any use whatsoever without the express written authority of GH. The report may only be reproduced and circulated in accordance with the Document Classification and associated conditions stipulated in this report, and may not be disclosed in any public offering memorandum without the express written consent of GH.

2. This report has been produced from information relating to dates and periods referred to in this report. The report does not imply that any information is not subject to change.

Key To Document Classification

Strictly Confidential	:	Recipients only
Private and Confidential	:	For disclosure to individuals directly concerned within the recipient's organisation
Commercial in Confidence	:	Not to be disclosed outside the recipient's organisation
GHP only	:	Not to be disclosed to non GHP staff
Client's Discretion	:	Distribution at the discretion of AES subject to contractual agreement
Published	:	Available to the general public

Revision History

Issue	Issue Date:	Summary
1.0	7/5/10	Original release – electronic copy only
2.0	15/5/10	Second release, following ETI's feedback on PM3 – electronic copy only

Circulation:	Copy No:
ETI	1
GH Bristol	2

Copy No: ____

CONTENTS

EXECUTIVE SUMMARY

This document outlines the issues associated with modelling a region of the wake behind a tidal turbine rotor, known as the near wake or the beginning of the far wake region. A review of the existing literature is presented which provides an overview of both the applicable modelling options and previous experimental campaigns which characterise the wake region of interest. The GH near wake model is described and the modelling approach justified.

The GH near wake model uses a semi-empirical approach to enable the initialisation of the GH far wake model. The key parameters which affect the model include: rotor thrust, ambient flow turbulence and the potential impact of bounding surfaces and/or other surrounding turbines. The model is used to predict the three dimensional flow field which is then passed to the GH far wake model as an input. The GH Blockage model feeds the model when appropriate, providing a corrected rotor thrust and an altered flow field around the turbine.

The GH near wake modelling theory is described in full with detailed derivations in the main document and in the supporting Appendices. A list of key assumptions that the GH near wake model makes is provided along with the relevant references to existing theory.

The method by which the mathematical models are implemented into a working code is described, as is the way in which the GH near wake model is to be incorporated within the GH TidalFarmer Beta code. Flow diagrams of the GH near wake model algorithms are presented and example outputs provided.

The PerAWaT work packages WG4WP1, WG4WP2 & WG4WP3 all provide experimental data to support the development and ultimate validation of the GH near wake semi-empirical model. The PerAWaT work packages WG3WP1& WG3WP5 will provide detailed CFD simulation results of the near wake region to further investigate the effects of bounding surfaces and provide additional validation of all three FDC.

SUMMARY OF NOTATION

Turbine characteristics

C_p	Power coefficient
C_{p0}	Power coefficient of the rotor in a boundless flow
C_t	Thrust coefficient
C_{t0}	Thrust coefficient of the rotor in a boundless flow
P	Power
P_e	Electrical power
T	Axial thrust on rotor
D	Rotor diameter
A	Area
hh	Hub height

Wake Field

B_w	Wake width
D_m	Velocity deficit
D_{mc}	Corrected velocity deficit
D_{mi}	Initial velocity deficit
D_w	Area averaged velocity deficit
EM	A constant value relating wake width to variance
I_{amb}	Ambient turbulent intensity
U_c	Wake centreline flow speed
U_i	Incident flow speed on rotor
U_o	Mean free stream flow speed
U_w (= u)	Wake flow speed
x_H	Length of the near wake

Constants

ρ	Density
μ	Dynamic viscosity
υ	Kinematic viscosity
g	Gravitational acceleration

Cartesian Co-ordinate systems

x	Axial co-ordinate
y	Transverse co-ordinate
z	Vertical co-ordinate

Abbreviations

1-d	one dimension (typically in the x-direction)
2-d	two dimensions
3-d	three dimensions
BEM	Blade element momentum
CFD	Computational fluid dynamics
FDC	Fundamental Device Concepts
RANS	Reynolds averaged Navier-Stokes

A general glossary on tidal energy terms was provided as part of WG0 D2 – “Glossary of PerAWaT terms”. This is a working document which will be revised as the project progresses.

1 INTRODUCTION

1.1 Scope of this document

This document constitutes the second deliverable (D2) of working group 3, work package 4 (WG3WP4) of the PerAWaT (Performance Assessment of Wave and Tidal Arrays) project funded by the Energy Technologies Institute (ETI). Garrad Hassan (GH) is the sole contributor to this work package. This document describes the theory behind and the method of implementation of the mathematical models used to evaluate the near wake forms behind a tidal turbine.

1.2 Purpose of this document

The purpose of WG3WP4 is to develop, validate and document an engineering tool that allows a rapid assessment of the energy yield potential of a tidal turbine array on non-specialist hardware. The specific objective of WG3 WP4 D2 is to both document and provide a technical justification for the use of the existing GH near wake model within the suite of models that make up the engineering tool 'GH TidalFarmer'.

1.3 Specific tasks associated with WG3 WP4 D2

WG3WP4 D2 comprises the following aspects:

- A detailed description of the theoretical basis of the GH near wake model
- A description of modelling methodology.
- A description of the method of integrating the GH near wake model into the GH complete engineering tool code.

1.4 WG3 WP4 D2 acceptance criteria

The acceptance criteria as stated in Schedule five of the PerAWaT technology contract is as follows:

D2: Near wake modelling report describes:

- How the existing GH near wake model is extended to incorporate different ambient flow conditions (turbulence intensity, bounding effects of the seabed and the free surface, and multiple wake interactions from the presence of other devices).
- The theory and methodology (assumptions and algorithms) behind the resulting near wake model.
- The method of integrating this model within the Beta code.

2 BACKGROUND

This section introduces the concept of a wake. A comparison between tidal and wind turbine wakes is presented which highlights the specific properties of tidal turbine wakes. A zonal model of a rotor wake is then presented, which introduces the concept of a "near" and "far" wake. The section concludes by commenting on factors which particularly affect the near wake.

2.1 General description of wakes

When flow passes a solid body, separation of the boundary layer from the surface occurs at some point. Downstream of the separation point the flow becomes disturbed by large-scale eddy motion. This region of disturbed flow, commonly referred to as the wake, is usually turbulent and has a different net axial velocity to the surrounding fluid (the free-stream), thus forming a shear layer. In time, turbulent mixing of the wake flow with the free-stream occurs until they merge, in such a way that conserves momentum (Tennekes 1972).

Figure 2.1 illustrates the streamtube that encompasses the flow which passes through the rotor swept area. The region downstream of the rotor is known as the wake. This is a turbulent region which has reduced axial velocity and static pressure compared with the fluid upstream of the turbine plane and is bounded from the outer (faster) moving flow by the vortices that are trailed from the blade tips.

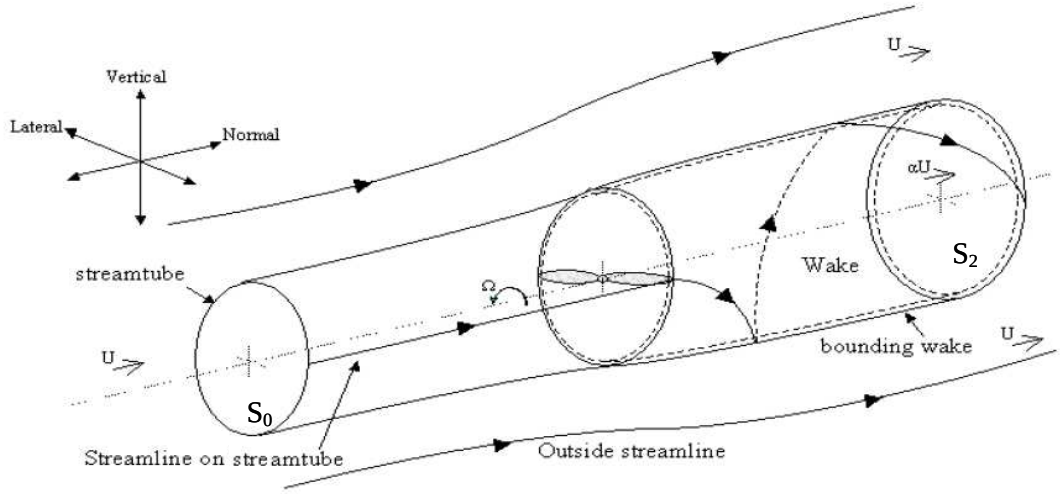

Figure 2-1 The near flow field in and around a rotor in an unbounded flow

2.2 Comparison between wind and tidal turbine wakes

The flow through and around a tidal turbine has many similarities with other commonly found rotors, in particular wind turbines. As for a wind turbine, the kinetic energy of the fluid (tidal stream) is converted into the rotational energy of the turbine, simultaneously driving a generator and thus creating electric power. Thake (2005) has shown that power performance of Marine Current Turbines' "SeaFlow" device (a 300kW prototype) demonstrates reasonable agreement with predictions from a blade element momentum (BEM) code. BEM codes are the design and prediction method that is used predominantly in the wind energy industry. This provides anecdotal evidence that process of energy (or momentum) extraction is very similar to that which is understood for wind turbines.

However there are some key differences been the flows that wind and tidal turbines operate in, these include:

- the presence of a bounding free surface (leading to blockage)
- additional types of flow unsteadiness (such as due to the effect of passing waves and different types of turbulence)

Cavitation is an added dynamic effect that has the potential to occur on parts of tidal turbines but is not a factor for consideration on wind turbines. However since cavitation will only have an indirect impact on the wake structure and since the majority (if not all) device developers are likely to design their devices to avoid the occurrence of cavitaton, due to its adverse impacts, it will not be considered further in this report.

There is also a concern that tidal flow turbulence characteristics may be shown to be site-specific, and thus be difficult to describe using standardised turbulence models, as discussed in the BERR report prepared by GH (2008). The differences between the flow environments that wind and tidal turbines operate within will lead to differences in the specific wake form and its evolution and these are discussed further in Section 2.4. Table 2.1 summarises the main parameters which characterise the flow environment and performance measurements of tidal and wind turbines.

As shown in Table 2.1 below at a typical rated flow speed (where the steady axial thrust is typically at a maximum) the power to axial thrust ratio is almost five times higher for the wind turbine than a tidal turbine (assuming the same power and thrust coefficients to equivalently rated wind and tidal turbines designed to generate that power for speeds of 12m/s and 2.7m/s respectively). Hence the forces experienced by a tidal turbine per unit radial span are going to be significantly higher than the equivalent forces experienced by a wind turbine for the majority of its working life-span. As a consequence modifications will be required to the structural design of the rotor blades compared with wind turbines, i.e. they will have a higher solidity and a thicker chord distribution. This will impact on the specific form of the near wake.

However, the ratio between the momentum deficit compared to the influx momentum in a tidal turbine wake is characterised by the thrust coefficient. Leading device developers such as TGL, MCT and Hammerfest Strøm all report similar thrust coefficients to wind turbines. Some device developers are pursuing different operating philosophies such as stall regulated or over-speed operation (or even rating at the peak flow speed), which is in contrast to the more-or-less wind industry standard operating philosophy of pitch regulation.

Global constants		Air [1]	Water[1]		Ratio A/W
Gravitational acceleration	g	9.81	9.81	m/s^2	1.00
Density	ρ	1.225	1000	kg/m^3	0.0012
Dynamic viscosity	μ	1.79E-05	1.14E-03	kg/ms	0.016
Kinematic viscosity	υ	1.46E-05	1.14E-06	m/s	12.38
Environment					
typical rating velo (hh)	U_o	12.0	2.7	m/s	4.51
typical mean velo		10	1.5	m/s	6.67
typical extreme		70	4.5	m/s	15.56
ratio mean to extreme		7	3		2.33
ratio rated to extreme		5.8	1.7		3.45
boundary layer					
height to free stream flow		2,000	44		
Re BL		4.59E+07	5.03E+07		0.91
typical roughness (sand)		0.0003	0.0003		
typical power law (sand)		0.1000	0.1429		
angle of slope for separation		<17'			
Typical characteristics for a 1MW device					
Turbine diameter (length-scale)	D	50	18	m	2.78
Swept area	A	1963	254	m^2	7.72
Thrust coefficient	C_t	0.89	0.89		1.00
Power coefficient	C_p	0.5	0.45		1.11
Rated power electrical	P_e	1.00	1.00	MW	1.00
Rated power mechanical	P	1.10	1.10	MW	1.00
Rated thrust	T	163	735	kN	0.22
Rated power to thrust ratio	P/ T	6.7	1.5		4.50
Rated impedance (T/ U_o)	Im	13,623	276,234	kg/s	0.05
Rated momentum flux		93	3,610	kg /ms2	0.03
Typical hub height		50	20		
Peak steady tower bending moment		8169	14699	kNm	0.56

Table 2-2 Numerical comparison of tidal and wind turbine parameters

2.3 Rotor wake regions and profiles

The specific form of a wake is likely to be complicated and device specific. Lissaman (1977) pioneered the transfer of profiles describing the decay of turbulent jet flows (Abramovich 1963) to their application in describing wind turbine wakes, providing a mathematical description of the wake. Lissaman (1979) proposed a model for a wind turbine wake, which as demonstrated in figure 2.2, subdivides the wake into three zones:

- Near
- Transient
- Far wake

As discussed in the previous section, tidal turbine wakes have many similarities with wind turbine wakes, hence the same model is applicable. GH TidalFarmer, along with many other established semi-empirical models for modelling array effects on wind turbines, is based on

[1] Conditions at 15˚C and 101.3 kN/m^2. NB. Values for sea water will be slightly altered due to salinity.

Lissaman's zonal description of the wake; hence the model an overview of the model is presented here.

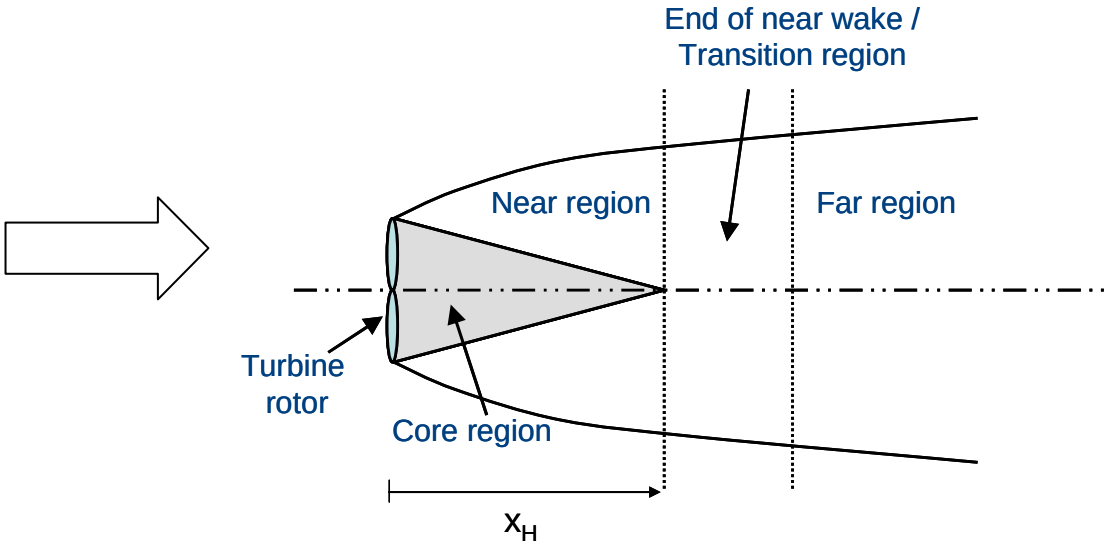

Figure 2.2 Wake structure, as proposed by Lissaman (1979)

Near wake: The near wake is the region immediately downstream of the rotor in which the specific properties of the rotor can be discriminated, such as the number of blades, tip vortices and stalled flow. The extraction of momentum from the flow, whilst conserving mass, drives a wake expansion, which also occurs in this region (usually within 1D downstream). The vortical structures which are trailed and shed from the blades and the device support structure comprise the wake and this region is bounded from the outer (faster moving) free-stream fluid by the vortices trailed from the blade tips and shed from the support structure. As discussed by Smith et al (2006), the near wake contains a "core" region in which constant velocity is assumed. The large velocity gradient at the edge of this area together with the tip vortices generates the additional turbulence in the wake. This additional turbulence, in conjunction with the ambient turbulence, increases the shear layer thickness with downstream distance, and at a certain distance downstream the shear layer reaches the wake axis. This marks the end of the near-wake region.

End of the near wake / Transition region: A review of literature from the wind energy sector suggest that the length of the near wake is open to debate in the e.g. Quarton and Ainslie (1990) suggested that the length of the near wake varies between 2D and 4D, whilst Crespo and Hernandez (1996) recommended a length of between 1D and 3D downstream. Another name for this region is the transition region i.e. the region which marks the end of the near wake and the beginning of the far wake where the wake can be said to be fully developed. This transition region is small and exaggerated in the schematic given in figure 2.2. For the purposes of PerAWaT this transition region will referred to as the "end of the near wake".

Far wake: Once the initial conditions for the far wake are established by the near wake region there are two main mechanisms that drive the wake structure. These are convection and turbulent mixing. If the fluid were completely inviscid then a volume of slower moving flow would convect downstream at a slower rate than the free-stream flow. However, turbulent mixing is present and acts to re-energise the wake, breaking it up and increasing the velocity until, at a point far downstream, the mean velocity profile across the wake is similar

to the free stream. Thus the far wake region progresses from the near wake region expanding as the velocity deficit recovers.

Lissaman (1979) postulated three different profiles for the near, transition and the far wake regions. For the core region he selected a box shaped profile (often referred to as a “top-hat”), for the near wake and the end of the core region (i.e. the transition) the profile has a blunt bell shape and for the far wake region a bell shape similar to a Gaussian profile. The various self-similar wake profiles suggested by Lissaman are shown in Figure 2.3. This figure shows profiles in the initial (near) region, one while the core is still present and the other at the end of the initial region. Also shown are a typical transition profile and a far wake profile. It should be noted that both radius and velocity deficit have been normalized in the figure. The centreline deficit is determined by the momentum integral which represents the axial momentum deficit extracted by the turbine. The assumption of self-similar profiles in the two major regions, means that the flow field is fully characterized by the velocity and radius scale so that it is only necessary to know the rate of wake growth to have full mathematical description of the flow field. The rules which determine the wake width are analytical as they follow as a direct consequence from the assumptions of profile and momentum conservation.

It is the focus of this report to detail the model employed to represent the near wake region, by which we mean the end of the near wake region and beginning of the far wake

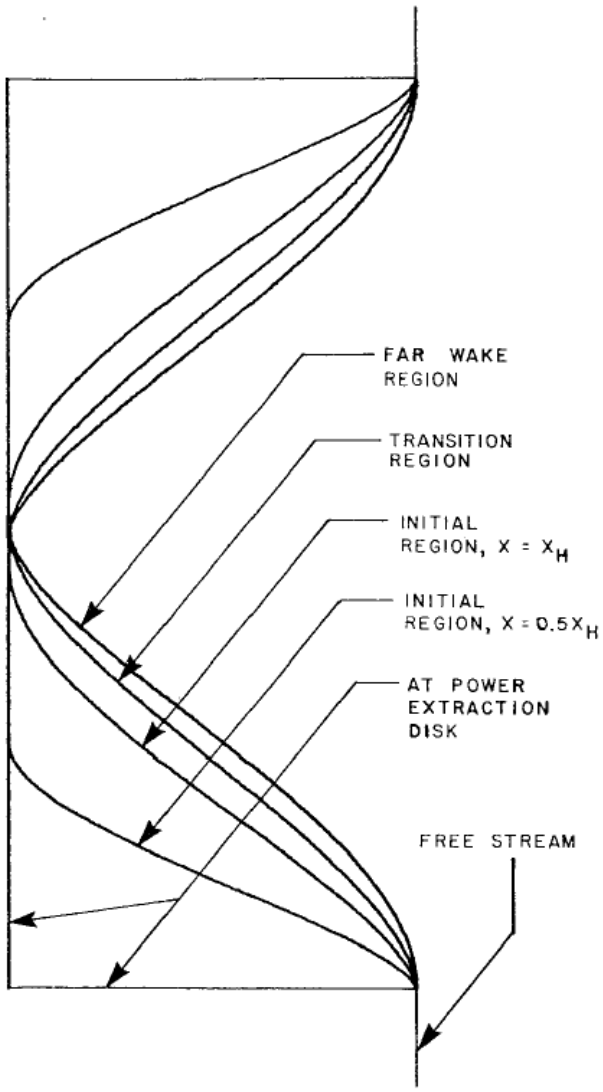

Figure 2.3 Normalised velocity profiles in the various wake regions. Reproduced from Lissaman (1979)

2.4 Factors affecting the near wake of a tidal turbine

The main factors which will affect the near wake of a tidal-stream turbine include:

- The amount of energy extraction
- The specific rotor geometry – e.g. number of blades, load distribution, hub size
- The operating speed of the rotor
- Ambient flow conditions, including those generated by the rotor support structure
- The presence of bounding surfaces
- Proximity to a free-surface

Some of these effects are illustrated in figure 2.4 and the potential effects of these parameters are detailed in this section.

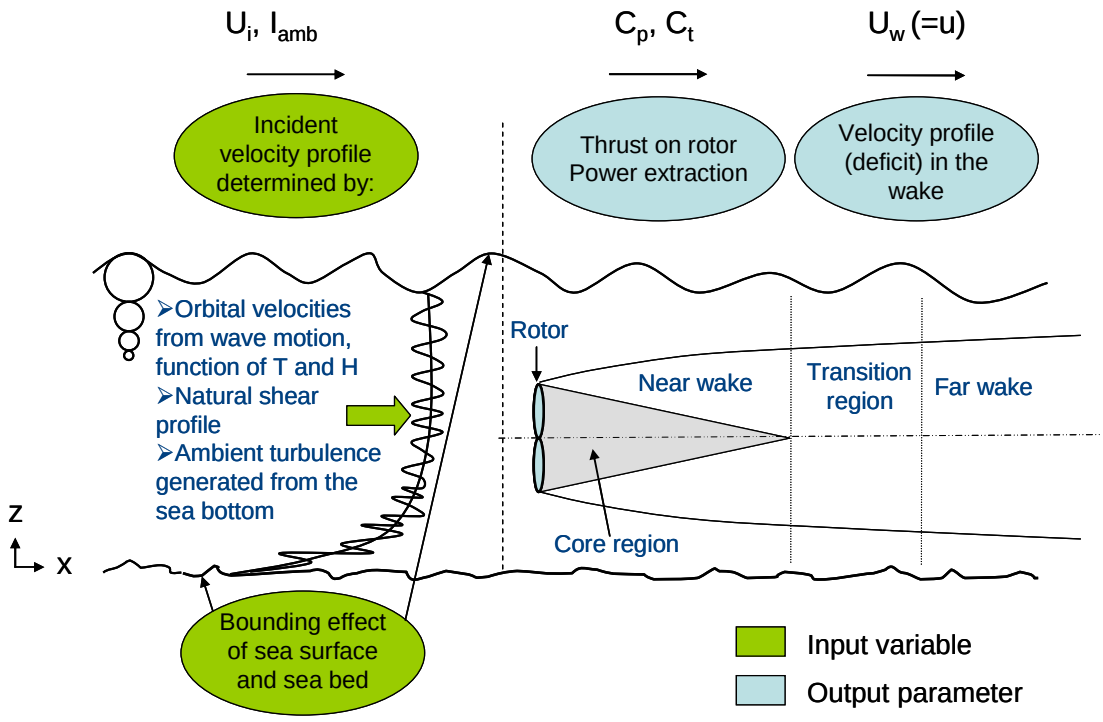

Figure 2.4 Variables affecting device performance and wake structure.

The amount of energy extraction as a percentage of the influx energy is a function of the operating point of the turbine i.e. the specific point on the performance curve (C_p and C_t as a function of tip speed ratio). Results from the ENDOW project (Barthelmie et al. 2003) suggested that lower thrust coefficient values result in less velocity deficit and hence less mechanical generated turbulence (shear) added in the near wake. However there is some non-linearity in the thrust coefficient, which is a function of the shape on the performance curve, therefore this may not be a general rule. And there is some evidence that passed the rated flow speed point, the wake velocity deficit is also function of the power coefficient. The ratio of Power to Thrust is lower for tidal turbines and thus it could be that this effect is very small for tidal turbines. It is a core objective of the PerAWaT project to parameterise the near wake form.

The specific design of the blade (rotor geometry) is a function of many factors, firstly the operating philosophy i.e. stall, pitch, or over-speed regulation, followed by the number of blades and also the specifics of the hub and tip design to minimise losses. The blade shape will affect the relationship between rotor thrust and power extraction, it will also affect the load distribution along the blade which may impact on the shed vortices that make up a major part of the near wake. The number of blades has a direct impact on the specific blade design, and also on the number of trailing vortices. Similarly the operating speed of the rotor will impact the near wake structure, i.e. the greater the rotation speed of the rotor the more swirl will be carried into the near wake. Typically tidal turbines are designed to lower tip speed ratios, thus reducing the amount of swirl imparted into the flow as compared to wind turbines.

Different ambient flow conditions have varied effects on the near wake and the overall wake recovery, e.g.

- The amount of ambient turbulence intensity in a flow can significantly enhance the mixing process and hence speed up the erosion of the core region and hence the

downstream position at which the end of the near wake can be said to have occurred. Ambient turbulence intensity is prominently governed by the seabed roughness.

- Free-surface waves are another source of flow turbulence. Certain wave states and operating depths may significantly impact on the entire wake recovery process.
- There is little data on the general form of the boundary layer (shear profile) at tidal energy sites. Some evidence suggests (Thake (2005)) that the modified seventh power law is appropriate, but at other sites it might be different. Operating in the lower region of the boundary layer may lead to a significant asymmetry in the flow above and below the wake, leading to alteration in the near wake form.
- Large scale eddies are another source of turbulence which have the potential to introduce additional energy to the wake, potentially further aiding recovery.

The presence of a bounding free surface will lead to an altered flow field around the turbine which may impact on the wake recovery and/or other turbines, including the

- Local flow acceleration in the near wake due to blockage, which may act to alter the rotor operating state.
- Wake recovery and expansion: The flow velocity in the bypass region around the turbine (and hence the near wake) will be increased due to the restriction of two bounding surfaces. This leads to change in the velocity deficit compared with the same rotor operating in an unbounded flow, which in turn will have an impact on the rate of mixing between the wake and the bypass flow and the resulting wake recovery length scales.

The extraction of momentum from a tranquil free surface flow (i.e. Froude number < 1) results in the reduction of gravitational head i.e. a drop in water depth as the flow passes over behind the turbine (Whelan et al. 2009). Typically the Froude number is sufficiently small that the gravitational head loss is minimal; and in the case of an isolated turbine, where the blockage ratio effectively goes to zero, this effect is negligible. Anecdotal evidence to-date from prototype deployments (evidence from MCT's "SeaFlow" and "SeaGen") suggests that there is no obvious changing in free surface. However if the distance to the free-surface is small it might impact on the near wake form and this is a matter for investigation.

As explained in detail in Section 6, the primary objective of the GH near wake Model is to initialise the far wake modelling. Hence it is the investigation of the effects of the differences in the flow environment on the beginning of the far wake form and the identification of where the end of the near wake occurs which comprise a major objective of the PerAWaT project.

2.5 Ducted and open-centre turbines

The unducted 3-bladed horizontal rotor has emerged as the leading technology in the wind energy sector. Tidal stream energy conversion technology is at a very early stage of development and at present there is a multitude of different technological approaches towards capturing tidal-stream energy. More detail on the different fundamental device concepts (FDCs) currently being pursued has been provided in see WG0 D2. Within the PerAWaT project three fundamental rotor configurations have been selected for analysis:

- Three bladed horizontal axis axial flow turbine (three bladed turbine)
- Ducted horizontal axis axial flow turbine (ducted turbine)
- Open-centre horizontal axis axial flow turbine (open-centre turbine)

Literature on the specifics of the form of the near wake of either ducted or open-centre horizontal axis axial flow turbines is scarce. There is little doubt that the specific properties

of the near wakes of the 3 different FDCs will be different due to both the rotor and support-structure, however the far wake profiles are likely to be similar.

Figure 2.5 is a CFD plot of the expected wake form for a ducted rotor. The specific geometry of the duct (or diffuser) will affect the structure of the near wake, e.g. the amount of initial expansion and the persistence of the core region. The developers of ducted devices make many claims for the benefits of using a duct, and high on the list is the ability to capture additional flow at large yaw angles. The CFD plot provided in Figure 2.6 below illustrates this effect (the duct creating a lifting force). The near wake form becomes very asymmetric in such a scenario.

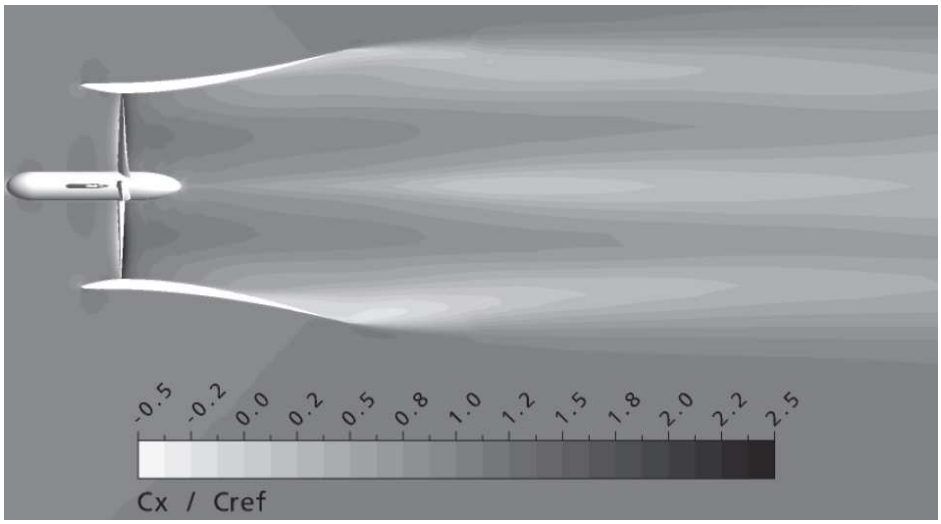

Figure 2.5 CFD (Ansys CFX) simulation of a ducted turbine. Reproduced from Münch et al. (2009)

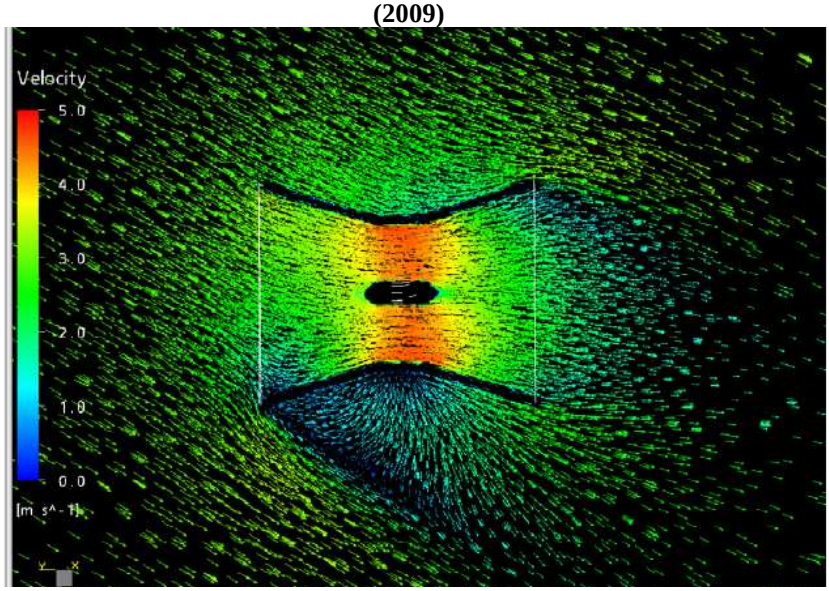

Figure 2.6 Effect of yawed flow on a ducted device (Ansys CFX). Reproduced from the Lunar Energy website.

It the purpose of experiments and numerical simulations being conducted as part of WG3WP1, WG3WP5, WG4WP1 and WG4WP3 to establish the key differences in the near wake between the different FDCs.

3 REVIEW OF RELEVANT MODELLING METHODOLOGIES

To date research into the analysis of tidal turbine specific effects, such as the effect of the bounding free surface and seabed and different ambient flow conditions on tidal turbine wake and its development has been limited. However a review of the literature reveals an extensive body of theory on wake modelling methodologies which can be adopted from the wind energy sector. Work on wind turbine wakes has led to models with varying degrees of sophistication. Complex field models at one of the spectrum attempt to model the wake of wind turbine using the fundamental equations of motion, at the other end of the spectrum empirical approximations are used in kinematic models to describe the wake. Outlined below are the four main theories associated with wake modelling. An initial description of these was provided in WG3WP4D1. Further description of the modelling method and the ability to represent the near wake is given in the following sub-sections:

- Actuator disc theory
- 3-d Potential flow methods
- Computational Fluid Dynamics (CFD)
- Semi-empirical wake models and simplified CFD methods

The review paper by Vermeer et al. (2003) provides a comprehensive summary of the existing modelling methods for wind turbine wakes and presents the fundamental equations upon which each method is based. This section prevents an overview of these modelling methodologies, each with varying computational requirements. The reader is directed to Vermeer's publication for more specific detail on these methodologies.

Traditionally, near wake research has been primarily focussed on assessment of performance and loading on a single wind turbine, while the far wake research has been more focussed on array effects. Because the near wake characteristics of the flow are initial conditions for the far wake, reference to the near wake in the work on the far wake is often made, and vice versa, hence it is difficult to draw an exact distinction between the methodologies employed for the near and far wake research.

3.1 Actuator disc methods

A commonly used model for the assessment of wind turbine performance is a 1-d (although assuming the wake is axisymmetric allows it to be considered 2-d) momentum balance of flow past an actuator disc in unbounded flow. The actuator disc distributes the loading of the turbine blades uniformly over a disc which acts as a discontinuity in pressure in the flow. Actuator disc theory is reviewed in many textbooks on helicopter and rotor aerodynamics. Mikkelsen (2003) provides a comprehensive review of actuator disc methods applied to wind turbines, in which the actuator disc concept has been used in combination with a variety of equations. Whelan et al. (2009) have used the actuator disc concept to develop a theory for the bounding effect of the free surface on tidal turbines.

The actuator disc concept assumes an ideal (inviscid) fluid and that the shear layer is infinitely thin. It provides a prediction of the speed in the wake at a single point downstream in the far wake, which is assumed to be the point prior to turbulent mixing; and results in the relationship that the velocity deficit at the disc itself is half that in the expanded wake. As such it can be used to correlate the performance of a turbine to the amount of expansion in

the wake, but it does not predict the flow field around the turbine. Actuator disc concept is the main building block of many methods for modelling turbines, in which it is combined with a viscous method. Blade Element Momentum theory (BEM) is the most commonly used method for modelling the performance and loading on rotors adopted for the commercial design of wind turbines, in which hydrofoil data and subsequent loading are determined iteratively by computing local angles of attack from the movement of the blades and the local flow field. The advantage of this model is that is it easy to implement on a computer, however similarly a BEM code does not provide any detail about wake development.

3.2 3-d Potential flow theory

Potential flow methods idealise the fluid to allow analytical solutions of the flow field around a body (such as a turbine) to be found. They vary in computational intensity from simple potential models in which the body is represented by a source or sink, to vortex wake models (panel methods and unsteady rotor lattice methods), which employ lifting line or surface theory to represent a body(s) in a flow e.g. a collection of sources or point vortices. The velocity at any point in the domain due to the distribution of sources, sink or vortices is then evaluated from Potential flow theory. N.B. The various actuator disc methods discussed in the previous section assume inviscid, incompressible and irrotational (i.e. Potential) flow, but are not defined here as a Potential flow method.

Vortex wake models can either have a prescribed (“frozen”) wake or compute the wake development as a part of the overall solution procedure (“free” wake). The difference in the wake models being that the “frozen" wake model in a uniform flow will simply move unaltered downstream with the advancement of the tidal stream, whereas in the “free" wake model the wake interacts with itself as the solution is stepped forward in time. In the frozen or prescribed vortex technique, the position of the vortical elements is specified from measurements or semi-empirical rules, making the technique computationally efficient, but limiting its range of application to more or less well-known steady flow situations. The free wake approach is more applicable for unsteady flow situations, complicated wake structures and general flow cases, such as yawed wake structures and dynamic inflow e.g. Simoes and Graham (1991). The disadvantage, on the other hand, is that the method is far more computational intensive than the prescribed wake method, because the Biot–Savart law has to be evaluated for each time step taken. Free wake methods also have disadvantage of having associated stability problems. Free wake models have been adopted widely in the helicopter industry (Leishman 2006).

3-d Potential codes are capable of modelling boundaries in the flow such as the free surface and seabed. Wang & Coton (2000) used a prescribed wake low-order panel method to investigate wall effects on wind turbine flows. However some form of empirical correction must be applied or artificial viscosity introduced in order to capture the initiation of the far wake e.g. using the velocity vorticity equations as discussed in Leishman (2006).

3.3 Computational Fluid Dynamics (CFD)

A computational fluid dynamics (CFD) code will be defined here as some code which computes the solution to the Navier-Stokes equations for a flow around a specified geometry and within specified domain. A variety of commercial codes exist (e.g. Ansys CFX) or they can be custom built, and they differ by the methods adopted to solve the equations, and both the types of mesh generator and turbulence models employed. However they all require the entire domain to be computed before a solution is arrived at. CFD codes range in computational intensity, from simplified CFD models coupled with other modelling

methodologies, to fully viscous computational fluid dynamics (CFD) simulations. The former can be quick to run but have uncertainties associated with the assumptions employed. The latter require a detailed set-up process and tend to have high computational power requirements.

A lack of reliable turbulence models and the difficulties associated with the prediction of laminar to turbulent transition, the high computational costs and the set-up complexities have led to limited use of fully viscous codes which provide a complete geometric description of the turbine for design purposes in the wind energy sector. Such methods have been more frequently been applied to detailed investigations, such as modelling the effects of complex geometries rather than looking at detailed structure of the near wake (e.g. Zahle et al. 2007).

Simplifications in the geometric representation of the turbine are frequently made to reduce computational time. For example Gant and Stallard (2008) used an actuator disc model representation of a turbine to investigate unsteady effects of tidal turbines. However this computation provided information on the far wake structure, rather than the near wake. Sørensen et al. (1998) combined the actuator disc representation with a 3-d Navier-Stokes solver and a BEM type technique in which body forces are distributed radially along each of the rotor blades in an attempt to study the effects of the wake dynamics and the tip vortices upon the induced velocities in the rotor plane. The main motivation for developing this model was to analyse and verify the validity of the basic assumptions that are employed in the simpler more practical engineering models.

CFD research which provides a “complete” description of the a wind turbine has taken place mostly through centrally funded collaborative projects, such as the EU project VISCWIND (Sørensen 1999), in which the participants have a comprehensive knowledge of CFD techniques, however such models have still tended to use a hybrid of Navier–Stokes free wake 3-d potential method in order to reduce computing time. No literature has been located in which a fully viscous “complete” model of a turbine has been produced. Figure 2.7 shows an image from an inviscid CFD computation which provides some information on the near wake structure. This computation was performed using the“PUMA2” code, which solves the Euler equations (the inviscid Navier-Stokes equations), Characteristics such as the number of blades can be identified up to half a diameter downstream from the rotor plane, however, no detail on the structure due to the shed vortices from the blade trailing edges is visible.

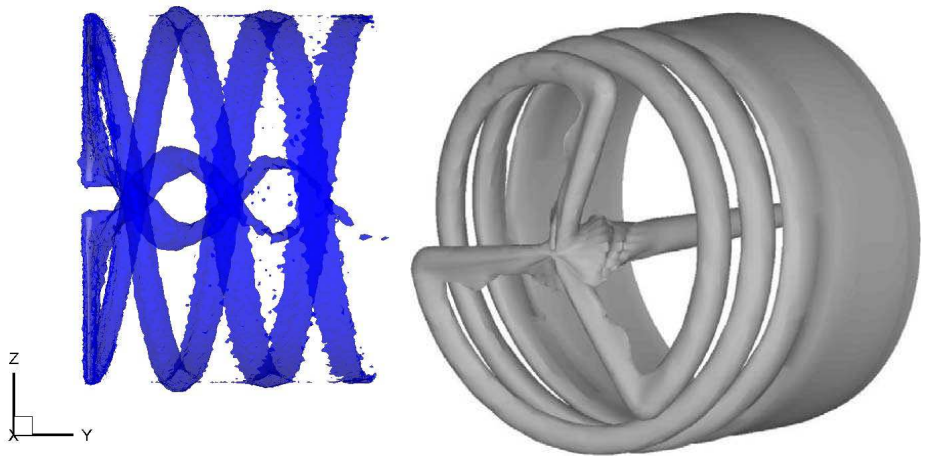

Figure 3.1 Instantaneous vorticity iso-surfaces, obtained from the PUMA2 project. Reproduced from Sezer-Uzol and Long (2006).

3.4 Semi-empirical models and simplified CFD methods

A variety of semi-empirical wake and simplified CFD models exist which have been adopted in the wind industry for prediction of wind farm effects, because they provide reasonable accuracy and are significantly less computationally demanding than either full CFD or 3-d vortex methods. These methods all have their origins in the work of Lissaman (1977) which was presented in Section 2.3. At the time when Lissaman first postulated the model for the different wake regions and profiles there was limited data from real wind turbines available for validation purposes. Since that time however this semi-empirical type of approach has been adopted in a variety of commercial codes that are used for the performance assessment of arrays of wind turbines e.g. GH WindFarmer (2010) which has undergone considerable validation (Tindal et al. 1993).

Semi-empirical models coupled with a CFD model are examples of rationalised modelling approaches. The aim of the semi-empirical model is to represent the initial form of the wake for subsequent far wake modelling. The key issue is to fully represent the factors which will impact on the far wake modelling. In the wind industry the parameters incorporated within the near wake semi-empirical model include: the turbine thrust; the ambient flow turbulence intensity and the wake width. The underlying theories behind these models are discussed in more detail in Section 6, and a brief overview of some of the different approaches that have been adopted are given below.

Wind industry standard models employ semi-empirical and simplified CFD models and range from being axisymmetric to 3-d and make varying assumptions for the profile of the velocity deficit in the wake regions. All the models described below solve a simplified form of the Navier-Stokes equations to account for the conservation of energy, mass and momentum in the flow and use an eddy-viscosity turbulence closure model to describe the mixing between the shear layer and the bypass flow due the ambient and added turbulence in the wake:

- Jensen's PARK model (described by Katic et al. 1986) is one of the simplest semi-empirical models adopted. It is axisymmetric and assumes a rectangular ("top-hat") velocity deficit. This model is known to produce significant discrepancies with measurements in the near-wake region due to the rectangular distribution; however the accuracy it provides in predicting the energy output is surprisingly high. Hence the model is commonly adopted in commercial codes which require a large number of calculations (e.g. such as those requiring computational for a large number of different flow directions).
- Ainslie (1988) first proposed the prototype of the model that is used today in almost all industrial software packages for wind farm design, such as in GH Wind Farmer (2010). This model is axi-symmetric and assumes a Gaussian profile as the inflow condition which initialises the far wake model. A comprehensive study was undertaken by Hassan (1993) which allowed systematic validation of Ainslie's approach.
- Crespo et al. (1994) proposed the UPMPARK model, which is based on the UPMWake model (Crespo et al 1988). This model assumes a Gaussian profile in the far wake, but it is 3-d. (elliptical). As a result it is computationally the most demanding of the three semi-empirical models presented here. Validation of these methods is discussed in provided in Crespo et al. (1999).

3.5 Summary of relevant modelling methods

Table 3.1 provides a summary of the different modelling methodologies presented in this section. Actuator disc theory is based on the assumption of an ideal fluid and can be used to correlate the performance of a turbine to the amount of expansion in the wake, but it does not predict the flow field around the turbine. Both Vortex and CFD are useful in the investigation of blockage and ambient flow effects on the near field wake structure. As part of the PerAWaT project several CFD models will be developed (WG3WP1 and WG3WP5) and used to investigate the impact of blockage and ambient flow effects on the near field wake structure. These results will inform the GH near wake model.

Table 3-1 Summary table comparing modelling methodologies

Existing model	Advantage	Disadvantage
Actuator disc theory and BEM models		1-d analysis is too simplified to represent the end of the near wake sufficiently. Only provides information at one assumed location in the wake of a turbine. Provides no information on the flow acceleration outside of the streamtube.
3-d Potential flow methods	Proven method in the wind industry (good correlation to wind tunnel experiments). Models predict the effect of rotor operating state, geometry, and could be developed to incorporate the impact of the free surface.	Not insignificant computational effort. Require corrections for the prediction of viscous effects.
Computational Fluid Dynamics Methods	Removes the need to explicitly model the near wake region, but retains the key parameter dependence.	Very sensitive to set-up (selection of most appropriate turbulence model etc.). Models require device specific calibration. Very computationally expensive.

To maximize the energy yield from a farm of turbines, the inter-array flow field must be predicted for numerous permutations of array design layouts. An optimisation code must be able to evaluate the downstream impact of tens of turbine wakes with varying flow speed and direction. For this reason an efficient computational numerical model is essential. The complexity and intensive computational requirements of both fully viscous “complete” CFD and 3-d vortex models precludes their direct use in an engineering tool, such as GH TidalFarmer. Instead a rationalised approach is preferred to form the basis for wake model GH TidalFarmer taking the form of the semi-empirical model developed by Ainslie (1988). As has been discussed in this section, semi-empirical models have been widely adopted in the wind energy sector for performance prediction of arrays of turbines. A review of the related experimental work conducted in this field, which is provided in the next section, confirms that such semi-empirical models provide reasonably accurate predictions of rotor performance when compared to more complex methods. The theory behind this model and how it has been and will be adapted in the development of GH TidalFarmer is discussed in sections 6 and 8.

4 REVIEW OF RELEVANT EXPERIMENTAL WORK

To date there are no (publically available) full scale measurements of tidal turbine wakes (near or far). The authors were previously involved in an experimental testing programme of tidal turbines (TSB project #200018), summarised in papers by Myers et al. (2008) and Bahaj et al. (2007), which is discussed in detail in Section 8. A review of the literature again reveals that the most applicable set of experiments that have been conducted to date have been in wind energy sector. This section discusses some examples of these.

4.1 Wind turbine near wake experiments

The review paper on wind turbine wake aerodynamics by Vermeer et al. (2003) also provides a comprehensive summary of near wake experiments. Data is available for both full and model scale wind turbine experiments investigating the near wake. However as discussed by Vermeer, good near wake experiments are hard to find in wind energy research. Given the complexities in the near wake, model scale experiments are preferred because of the ability to create a controlled environment. Again, the reader is directed to Vermeer's publication for more specific detail on these experiments.

The porous disc analogue of a rotor has been frequently used to experimentally simulate far wakes of rotors. Sforza et al. (1981) were some of the first researchers to use the analogy for modelling horizontal-axis rotors. The near wake of a porous disc immersed in an axial flow is clearly unrepresentative of a wind or tidal turbine, due to the small scale turbulence, however good agreement has been shown in the far wake. Myers et al. (2008) used porous discs to simulate the far wake of an array of tidal turbines and suggest that the near wake specific parameters, such as swirl and shed vortices, have little bearing upon wake re-energisation and have usually dissipated by approximately 4 diameters downstream.

Magnusson (1999) compared full scale measurements in the near wake to a simple numerical model. His work highlighted the uniqueness of each near wake region and emphasised the need for measurements of velocity profiles (i.e. transects across the wake) rather than just measurements at the centreline in order to correctly inform numerical models. Medici and Alfredsson (2004) measured the velocity deficit at various axial positions in the near wake of a model scale wind turbine. The results of some of these tests are shown in figure 4.1, in which U/UO is the wake velocity normalised by the upstream velocity. A Gaussian type distribution is shown to occur at 3 diameters downstream from the turbine plane (x/D = 3D). Figure 4.1 also provides insight into the effect of ambient turbulence, suggesting that increased turbulence intensity leads to a quicker recovery of the velocity deficit.

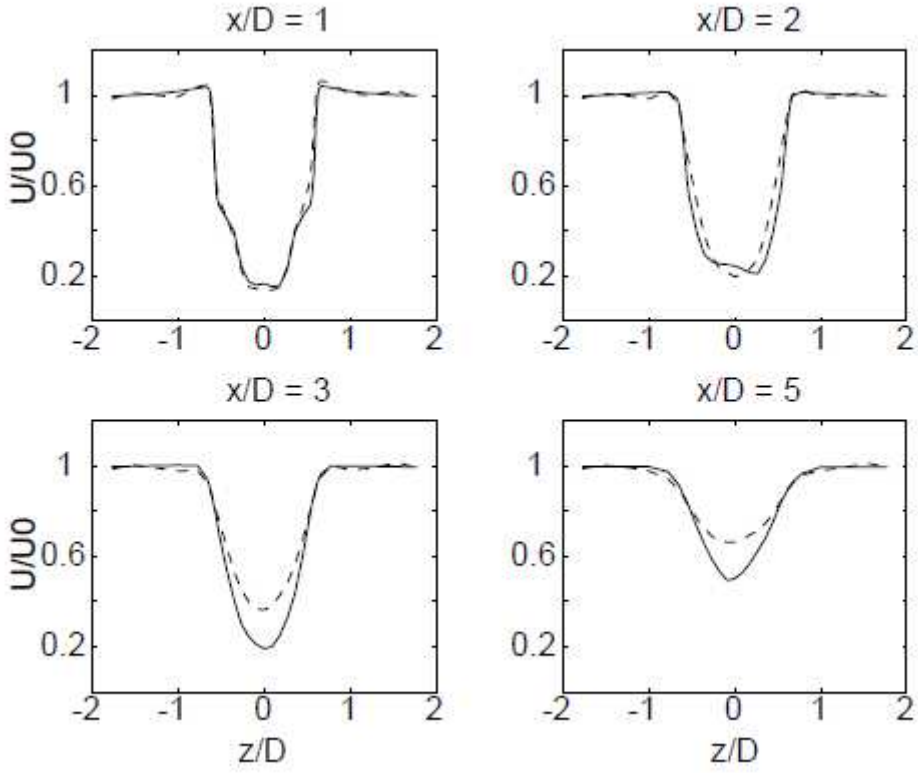

Figure 4.1 Difference between the streamwise velocity without free-stream turbulence (solid line) and with turbulence (dashed line). Reproduced from Medici & Alfredsson (2004).

4.2 Experimental validation of existing semi-empirical and simplified CFD models

The semi-empirical wake models and simplified CFD models widely adopted by the wind energy sector for commercial purposes have been explicitly and implicitly verified by accurately predicting wind speed in the far wake of wind turbines and the power production of wind farms for many years (Tindal et al. 1993). The ENDOW project (summarised in Barthelmie et al. 2003) provided validation of a variety of models. Figure 4.2 shows that the GH WindFarmer (labelled "GH") is shown to give good agreement with measurements (labelled "SMS vs LMS") in the far wake region (9.6 diameters downstream of a specified turbine).

Figure 4.3 shows the results of a validation study of GH WindFarmer. It demonstrates good agreement between the measured data and the GH near wake model prediction. As previously mentioned, a comprehensive study was undertaken by Hassan (1993) which allowed systematic validation of GH WindFarmer model. The array experiments which are planned as part of PerAWaT (WG4WP2) have been designed taking into consideration the learnings from this extensive former validation exercise.

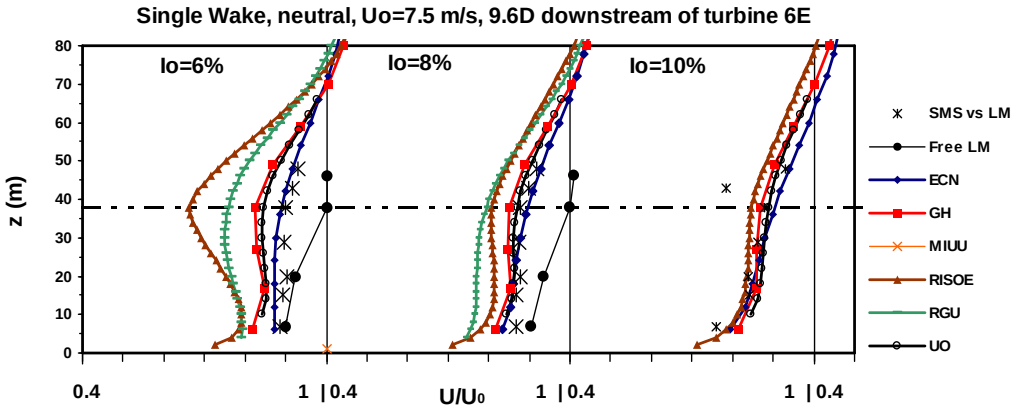

Figure 4.2 Experimental data and wake models for the single wake case. Measurments are denoted by –x-. Reproduced from Barthelmie et al. (2003).

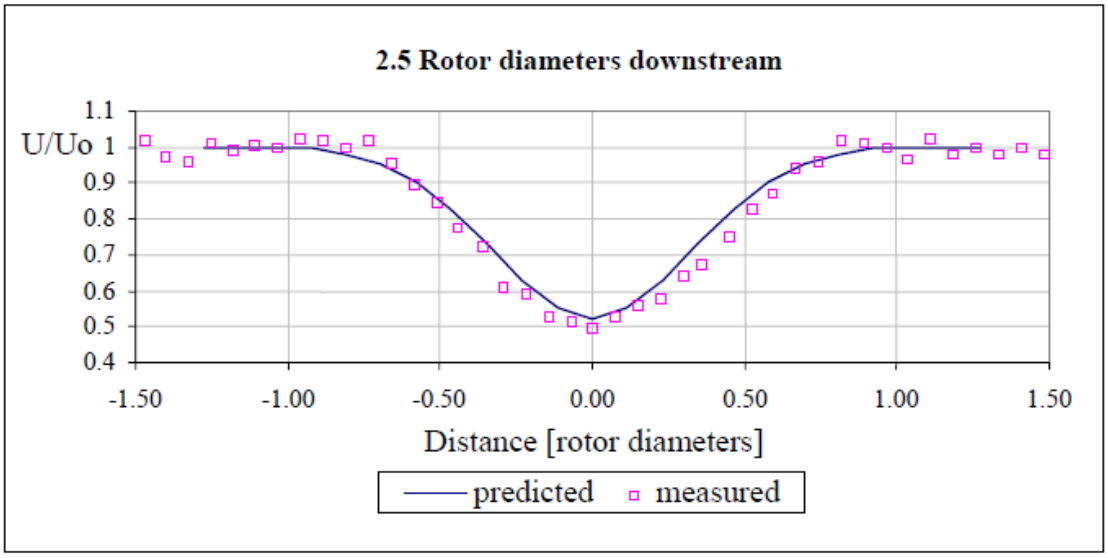

Figure 4.3 Comparison of GH Eddy Viscosity Model with wind tunnel measurements at 2.5 Rotors downstream. Reproduced from the GH WindFarmer Validation Manual (2003).

5 THE GH NEAR WAKE MODEL

This section introduces the GH near wake model and the reasoning behind it.

The purpose of the GH near wake modelling is not to predict the change in wake form as the wake changes at different downstream locations, but to describe the wake form at the beginning of the far wake region in order to initialise the far wake model.

5.1 GH modelling philosophy

GH's modelling philosophy is to provide engineering solutions to meet a commercial need, and in the case of tidal array design this means providing a design tool that can offer practical solutions to aid the iterative design process. To develop an appropriate design tool, rationalised modelling methods based on a physical understanding of the Navier-Stokes equations that provide robust estimates with known uncertainties are preferred to more complex numerical methods.

5.2 Description of the GH near wake model

The GH near wake model uses a set of equations to model the flow inside the wake at the end of the near wake region/beginning of the far wake region. The model is based on a fundamental understanding of the hydrodynamics of rotors as they extract momentum from the flow and flow dynamics. Coupled with experimental tidal and operational wind turbine wake data a semi-empirical model to describe the wake form in at the beginning of the far wake region has been developed.

The GH near wake model incorporates the effect of several key parameters:

- Turbine operating state in the form of thrust coefficient
- Ambient flow conditions
  - Incident flow onto rotor
  - Turbulence intensity
- Bounding effects from the seabed, free-surface and other turbine wakes.

A detailed description of the theory behind the model is given in Section 6 which further explains how the parameters listed above are incorporated into the model.

.

5.3 Justification for the rationalised modelling approach

The Actuator disc and BEM methods do not model the flow field around the rotor and are of limited use for the purpose of the characterising or modelling the near wake. In comparison CFD and vortex lattice methods can be used to model the detailed effect of changing the flow direction onto a specific blade geometry. However, both are too computationally intensive for the purpose of an array design tool. Typically CFD is used at the validation stage of a design, or when better understanding of complex fluid/structure interaction is required. Evaluating the array flow field using CFD to model each rotor is a hugely complex and very computationally expensive task.

The table below highlights the change in order of magnitude of computational effort with modelling an increased definition of the rotor. Although the most simple of Vortex methods might be computationally feasible, the practical process of setting-up the model makes this method unattractive for an array design tool.

Table 5.1 Typical computation times source [Li et al. (2007)]

Method	**Time[s]**
Parametric model	<0.1s
Vortex method (free-wake 2D)	1e4
Vortex method (free-wake 3D)	1e5
CFD – RANS (Fluent) 2D	1e6
CFD – RANS (Fluent) 3D	>>1e6

Thus the objective of near wake modelling for use in an array tool must be to produce a parametric model which can feed either a detailed or rationalised CFD model. The GH near wake model is focused on using fundamental understanding, experimental and full scale data, and available detailed CFD simulation results to develop a suitable parametric model. Hence the aim of the GH near wake model is to be of sufficient complexity to incorporate the key factors which impact on far wake modelling.

The evidence from the wind industry is that the wake modelling in the areas of interest (i.e. the far wake) is a function of two key parameters; rotor thrust and ambient turbulence intensity of the flow.

6 GH NEAR WAKE MODEL THEORY

The GH near wake model is based on a semi-empirical model first proposed by Ainslie (1988) that was first presented in section 3.1.4. It is based on the idea of separate near/far wake modelling. The near wake model is used to initialise the far wake model.

This section details the fundamental assumptions upon which a semi-empirical model is developed leading to a mathematical description of the near wake profile. The section concludes with the key developments to-date of the GH near wake model to account for the tidal environment.

6.1 Fundamental understanding

The semi-empirical model developed by GH for wake model is based on the following fundamental assumption that momentum is conserved within a control volume (shown in the Figure 6.1) during the energy extraction process:

Momentum deficit in the wake = Momentum flux in inflow - Momentum flux in outflow

And that the

Momentum deficit in the wake = Thrust on rotor

Using actuator disc theory to describe the thrust on the rotor, the momentum deficit can be described as.

$$\int_v \rho U_i \nabla U_i dV - \int_v \rho \underline{u} \cdot \nabla \underline{u} dV = \frac{1}{2} \rho C_t S U_i^2 \qquad (6.1)$$

Where U_i is the uniform upstream velocity and $\underline{u}$ is the downstream velocity field. Assuming the flow is incompressible and applying the divergence theorem, the above equation becomes:

$$\rho \int_{A_i} U_i^2 dA_i - \rho \int_{A_r} \underline{u}^2 dA_r = \frac{1}{2} \rho C_t S U_i^2 \qquad (6.2)$$

Actuator disc theory applies a 1-d analysis to describe $\underline{u}$ as a linear function of the upstream velocity, i.e.

$$\underline{u} = U_w = \alpha U_i \qquad (6.3)$$

Combining equations 6.2 & 6.3 can be reduced to the well known equation:

$$C_t = \left(1 - \alpha^2\right) \qquad (6.4)$$

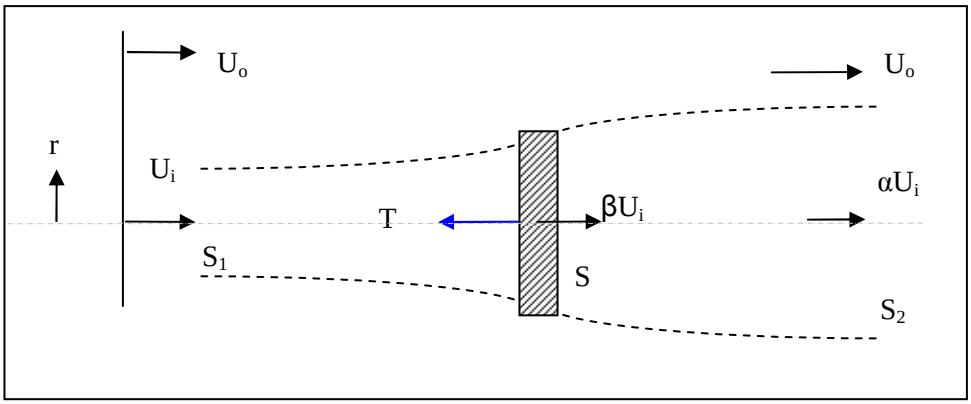

Figure 6-1 Schematic of 1-d wake flow

Defining the velocity deficit in a non-dimensional form, then

$$D_w = 1 - \frac{u}{U_i} \qquad (6.5)$$

Combining 6.5 and 6.3 leads to

$$D_w = 1 - \alpha \qquad (6.6)$$

Then substituting into Equation 6.4 leads to

$$C_t = D_w\left[2 - D_w\right] \qquad (6.7)$$

Which rearranged and solved for D_w yields

$$D_w = 1 - \frac{U_w}{U_i} = 1 - \sqrt{1 - C_t} \qquad (6.8)$$

where D_w is the area averaged velocity deficit in the wake. This equation is the basis of the relationship between the wake velocity and the turbine operating state. However, as the experimental and numerical models show the pressure driven wake flow quickly breaks down from the 1-d top-hat model and the velocity distribution in the near wake is better described by a Gaussian profile (as shown by Lissaman in Figure 2.3).

6.2 Development of a semi-empirical relationship

Significant work by the Central Electricity Generating Board (CEGB) in the early work on wind turbine wakes analysed experimental wake data to derive a set of semi-empirical equations which describe the initial far wake profile at a distance of 2D behind the turbine Ainslie (1985). The wake data showed that the decay rate in the far wake is comparatively insensitive to the initial velocity profile and that using a Gaussian profile at the near wake is more than adequate to capture the dominate factors which affect far wake modelling. Figure 6.2 below illustrates the use of a Gaussian profile.

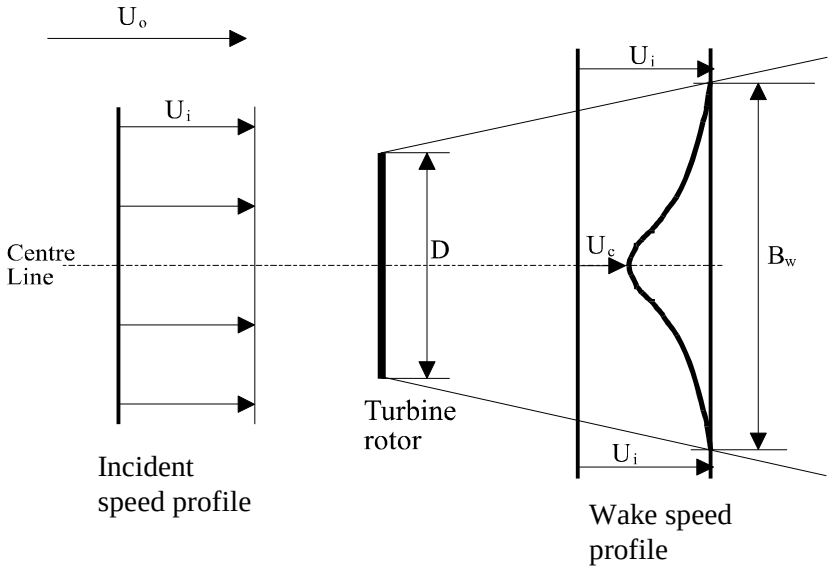

Figure 6-2 Gaussian profile describing the wake form

In low ambient wind flow the centreline velocity deficit (D_m), or peak of the Gaussian profile, was show to be solely a function of the turbine thrust and the actuator disc model above was corrected with empirical data such that

$$C_t = 4.2 D_m [2 - D_m][0.14 - 0.125 D_m]/[1 - D_m] \qquad (6.9)$$

Which leads to the cubic equation in D_m

$$D_m^{\,3} - 3.12 D_m^{\,2} + 1.905(1.176 + C_t) D_m - 1.905 C_t = 0 \qquad (6.10)$$

Solving for D_m leads to

$$D_m = C_t - 0.05 - \left[(16 C_t - 0.5)\right] \qquad (6.11)$$

To ensure that momentum is conserved the width of the wake must be set such that the momentum deficit described by the axis-symmetric Gaussian profile. The following section derives the wake width to ensure momentum in the wake is conserved.

Conserving mass,

$$\rho \int_{A_i} U_i \, dA_i = \rho \int_{A_r} u(r) \, dA_r \qquad (6.12)$$

Then Equation (6.2) becomes

$$\rho \int_A \left(U_i^{\,2} . \frac{\underline{u}}{U_i} - \underline{u}^2 \right) dA = \frac{1}{2} \rho C_t S U_i^{\,2} \qquad (6.13)$$

Or in cylindrical coordinates

$$\int_0^{2\pi}\int_0^{\infty} U_i\, u(r) - u(r)^2 r\, dr\, d\theta = \frac{1}{2} C_t S U_i^{\,2} \qquad (6.14)$$

Assuming an axis-symmetric Gaussian profile which can be described by

$$f(r) = C.e^{-\left(\frac{r^2}{2\sigma^2}\right)} \qquad (6.15)$$

Where σ is the variance of the distribution and *C* the peak. Appling this to Equation 6.5 (where $D_w = D_m$) yields:

$$1 - \frac{u(r)}{U_i} = D_m e^{-EM.\left(\frac{r}{B_w}\right)^2} \qquad (6.16)$$

Where $C = D_m$ and B_w is the wake width, and EM is a constant relating the variance to the wake width in the following way:

$$2\sigma^2 = \frac{B_w^{\,2}}{EM} \qquad (6.17)$$

Equation 6.14 then becomes

$$u(r) = U_i \left(1 - D_m e^{-EM.\left(\frac{r}{B_w}\right)^2} \right) \qquad (6.18)$$

Substituting Equation 6.17 into 6.14 and integrating yields leads to the solution for the wake width (a full derivation is provided in Appendix A):

$$\mathrm{B_w} = \sqrt{\frac{3.56\mathrm{C_t}}{8D_m(1-0.5D_m)}} \qquad (6.19)$$

Further work incorporating the effect of ambient flow turbulence (i.e. atmospheric boundary layers Ainslie (1988) developed on this work and proposed the following equation based on wind tunnel studies (Connell 1982 and Vermeulen 1980) of rotors for the for the initial centre line velocity deficit D_m, at a distance 2 diameters downstream, which is a function of the axial thrust and ambient turbulent intensity:

$$\mathrm{D_{mi}} = 1 - \frac{U_c}{U_i} = \mathrm{C_t} - 0.05 - \left[(16\mathrm{C_t} - 0.5)\mathrm{I_{amb}}/1000\right] \qquad (6.20)$$

Where I_{amb} is the ambient turbulence intensity of the flow.

The two equations above are the initial conditions used in the GH far wake modelling model. The far wake model is a simplified CFD solution the details of which are in WG3WP4D5.

There are some additional factors to consider which might affect the far wake modelling. One such consideration is the situation when on turbine is in the wake of another turbine. In this situation the initial wake velocity deficit needs to be corrected from the incident rotor flow speed to the free stream flow speed if there is sufficient available surrounding momentum. This correction is necessary in order to ensure that at distances far downstream, the wake flow speed will recover to the free stream value rather than that incident on the rotor. Therefore, the initial centre line velocity D_m is scaled by the ratio of the average influx velocity U_i and the free upstream flow velocity according to the following formula, to yield D_{mc} (the corrected velocity deficit):

$$D_{mc} = \left(1 - \frac{U_i}{U_0}\right) + \left(\frac{U_i}{U_0}\right) D_m \qquad (6.21)$$

The applicability of this correction in closely packed arrays needs revision, where the available surrounding momentum might be limited, e.g. in a blocked flow such as a tidal-stream site.

6.3 GH near wake model - adaption to tidal farms

The main consideration when adapting the existing wind semi-empirical model to the tidal environment is assessing the validity of using the available empirical evidence. This is one of the prime objectives of the PerAWaT device scale experiments. Previous research (Myers et al. 2008) suggests that the wake form is similar and that the semi-empirical relationship can be used. But this is only one data set and further experiments and simulations in realistic turbulence conditions are required (see Section 8 for more details). If the empirical data shows a different relationship, then the semi-empirical model must be altered.

In addition to assessing the validity of the empirical equation relating rotor thrust and ambient flow turbulence intensity to centreline velocity deficit, the impact of a different surrounding flow field must be considered. The main differences to consider are:

- Different flow unsteadiness and turbulence structures, such as large eddies forms and free-surface waves action, which may impact the initial wake form and its development
- The position of the wake within the boundary layer, which may lead to significant differences in flow above and below the wake
- The presence of a bounding free surface, which may lead to two effects
    - An altered relationship between the rotor thrust and the momentum deficit coupled with a local flow acceleration outside of the near wake region
    - The limitation of surrounding momentum to feed the wake recovery process

The first point will be addressed via the experimental and numerical investigations and it is expected that the ambient turbulence intensity value will be adjusted to incorporate these effects. The second point is to a degree addressed in the existing model by the normalisation of the inflow profile. However, a surrounding momentum assessment is incorporated into the model. This is detailed further below.

The third point is tackled in two ways. The correction of blockage effects is incorporated via the GH Blockage model. This predicts the change in relationship between the rotor thrust and the momentum deficit. It also predicts any change in flow around the wake. These aspects are fed into the GH near wake model to correct the initial velocity deficit (via Equation 6.19). The impact of boundaries to limit wake expansion has been addressed by developing the GH wake model to allow for a break in the axis-symmetric assumption. The wake models (both near and far wake) incorporate an elliptical Gaussian profile, allowing vertical wake width to be limited by the water depth. The Elliptical characteristics are derived from the GH Blockage model. The figure below illustrates the elliptical Gaussian profile.

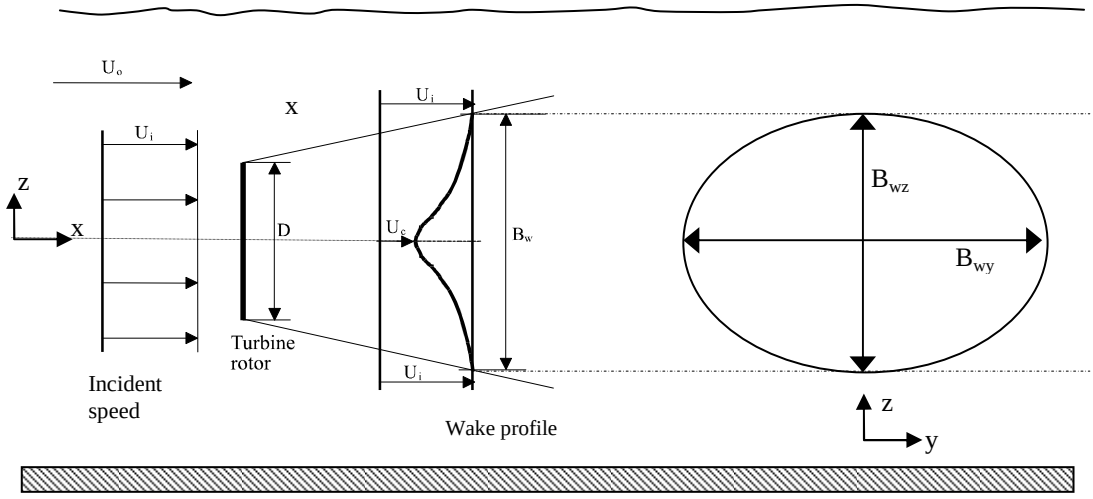

Figure 6-3 Elliptical Gaussian wake model

The analysis undertaken in section 6.3 is repeated for an elliptical Gaussian profile (and is provided in Appendix 2), leading to the following equation:

$$B_{wz}B_{wy} = \sqrt{\frac{EMC_t}{8D_m(1-0.5D_m)}} \quad (6.22)$$

The limited evidence to-date (Myers (2008)) shows that the elliptical model may not be needed for the "near wake model". It is the intention to further investigate this within the PerAWaT project, via CFD simulations and rotor experiments. The developments planned under PerAWaT are provided in section 8.2.

The adoption of the deficit correction model outlined in the section above and yielding Equation 6.21 can be discarded if a more rigorous approach to assessing the surrounding momentum is incorporated into the wake modelling. Evaluating the area-averaged momentum in the surrounding flow field allows the wake deficit to be corrected in a more robust manner. This also incorporates the effect of boundaries. The following table evaluates the extend of the surround area to be used to evaluate the area-averaged momentum.

Conserving momentum, assuming a top-hat profile (thus using Equation 6.5), the area occupied by the momentum deficit far downstream is:

$$A_{\text{downstream}} D_{w,downstream} \left[2 - D_{w,downstream}\right] = A_{\text{near}} D_{w,near} \left[2 - D_{w,near}\right]$$

Assuming the wake form is indistinguishable when the deficit is ~ 5%, the area downstream is approximately nine times that of the swept area. This equates to an area with three times the rotor diameter or a rectangle capped by a typical water depth of 2.5D and a width of 3D. Thus the inclusion of a fairly significant area is required. Further consideration must be given to the limiting of momentum for wake recovery from adjacent turbines.

The GH near wake model uses an ellipse area to evaluate the area-averaged momentum deficit. The ellipse coverage may extend beyond bounding surfaces or the reflection plane of adjacent turbines. In such cases the available momentum in these areas is set to zero. The area-averaged value then takes all available surrounding flow into account.

6.4 Summary the key assumptions

The main assumptions made in the GH near wake model area:

- The near wake model evaluates the wake form at the beginning of the far wake, from which point the wake recovery is predominantly independent of near wake effects.
- The wake decay rate in the far wake is comparatively insensitive to the initial velocity profile and that a Gaussian profile at the near wake is more than adequate to capture the dominate factors which affect far wake modelling.
- The near wake form is predominantly a function of the rotor thrust (coefficient), the ambient turbulence intensity. Correction for blockage effects will be incorporated via the GH Blockage model (see WG3WP4D1 for details).
- Momentum is conserved (i.e. no addition of momentum very large scale eddy motion in the near wake region).
- The wake has bi-symmetry allowing an elliptical Gaussian (or similar) form

7 GH NEAR WAKE MODEL METHODOLOGY AND IMPLEMENTATION

This section describes how the GH near wake model is incorporated into the GH TidalFarmer array modelling software tool.

The overall concept of the GH TidalFarmer modelling method is to reduce the extremely complex interactions between tidal turbines and the surrounding flow field into a distinct physical process which can be simplified and modelled. Classical analysis simplifies the physics process under investigation via the selection of an appropriate scale. The three appropriate scales of interest are Coastal basin, Array and Device scale. The GH near wake model is found at the "Device scale" level.

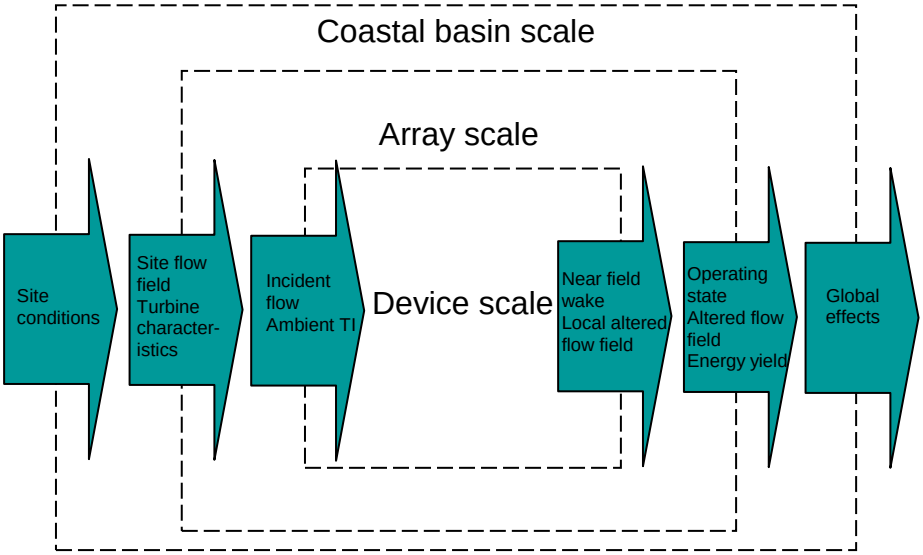

Figure 7-1: Hierarchy of modelling domains and scales

Within the "Device scale" level there are several mathematical models that are drawn upon. The figure below puts the GH near wake model into context within the GH TidalFarmer software.

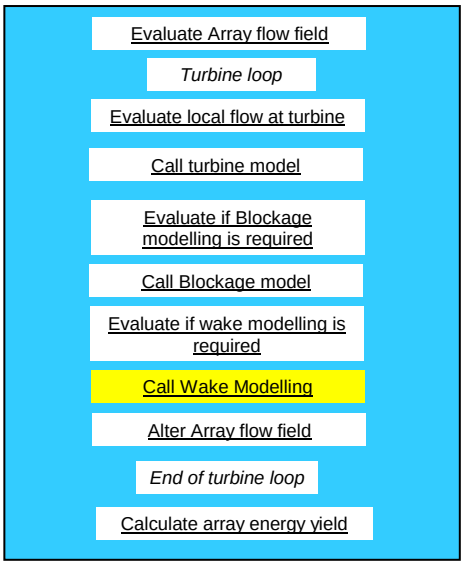

Figure 7-2: Overview of GH TidalFarmer software architecture showing the GH Wake model in its context

The sections below describe how the Wake model is incorporated in to the GH TidalFarmer software.

7.1 Near wake modelling

To evaluate the near wake profile in anticipation of the far wake modelling the following set of inputs are used:

- The operating thrust coefficient.
- The disc-averaged U_i incident speed at the rotor location.
- The ambient turbulence intensity (depth averaged value)
- Effective distances to boundaries with other turbines
- The surrounding flow field (in the plane of the rotor)
- Effect of blockage is incorporated using input from the GH Blockage model: If the Blockage model is run which is dependent on the position in the optimisation loop, then the additional inputs are provided
  - The Blockage corrected C_t
  - An altered flow field around the wake
- The required accuracy for the calculation (i.e. set the grid size and modelling method) based on the iteration point in the optimisation loop.

The main core steps are:

Within the turbine loop
- Calculate the centreline deficit
- Evaluate available surrounding momentum
- Correct for surrounding momentum
- Evaluate the wake width
- Evaluate the velocity deficit Gaussian profile

Figure 7.3 illustrates the near wake modelling processes and tables 7.1 and 7.2 provide a functional description of the GH near wake model including reference to the equations presented in section 6.

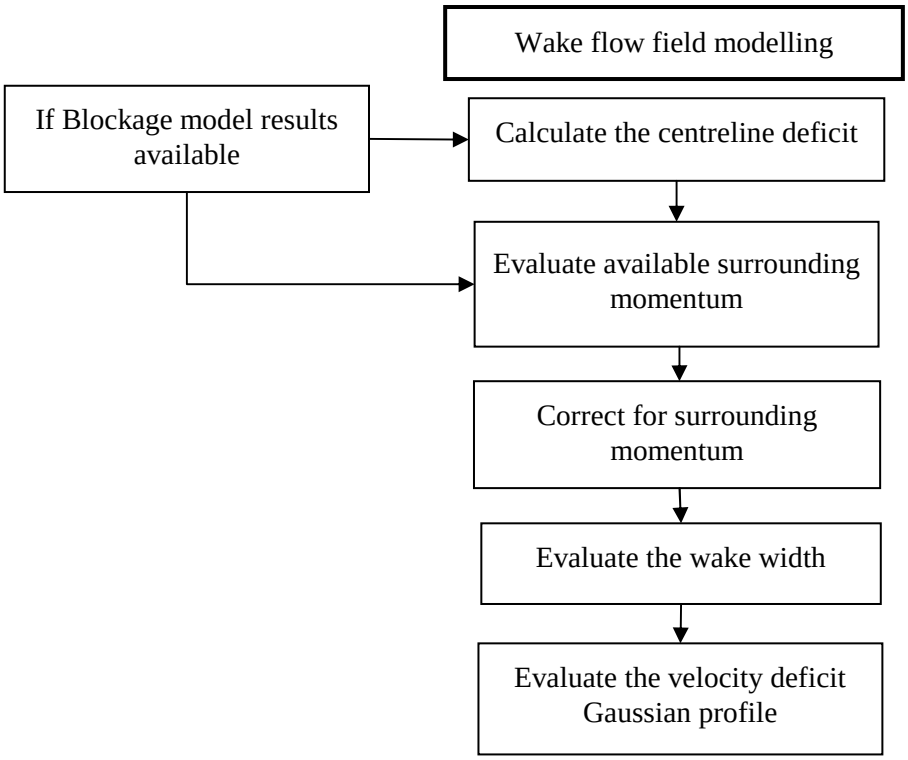

Figure 7-3 Flow diagram of the GH Wake model: Flow Field modelling

7.2 Implementation

The GH TidalFarmer software tool will consist of a single executable file (user interface) with which the user will interact, as well as a number of calculation modules which will be implemented as dynamic-link libraries (DLLs). Tidal calculations will be controlled and coordinated by a top-level "core functionality" module. The GH near wake model is likely to be implemented as part of the wake core functionality module, because near wake model is closely bound up with the main wake calculation in GH TidalFarmer.

Choosing the most appropriate programming language depends on the method of investigation and how the results will be analysed. Currently the code is written as a Matlab script, which allows for easy interrogation and analysis.

The user interface is likely to be written in a .NET language such as C#, while the modules which do the actual calculations will either remain in Matlab or migrate to another language, such as Fortran or C++. The wake-modelling subroutine will be called at the appropriate point in the speed, direction and optimisation loop.

Table 7.1 Summary functional description

Model	Inputs	Outputs	Method used
Near wake model	Turbine C_t Incident rotor averaged flow speed Ambient turbulence intensity	3-d wake velocity deficit profile	Semi-empirical equations 6.19&6.20 (to be checked via PerAWaT)
Blockage model	Incident 3-d flow field Boundless turbine characteristics (C_{p0}, C_{t0}) Turbine locations	Altered turbine performance characteristics (C_p, C_t)	Blockage performance model
		Altered 3-d flow field around turbine.	Blockage flow field model

Table 7.2 Detailed functional description of the near wake model

Task	Input	Output	Method
Feed in Blockage model data	Corrected rotor C_t	Updated C_t value	Checking algorithm
Calculate the centreline deficit	Rotor C_t value Ambient Turbulence intensity value (dept averaged)	Centreline velocity deficit	Equation 6.20.
Evaluate available surrounding momentum	Surrounding flow field (corrected for blockage if available) Proximity to boundaries and other turbine wakes	Equivalent free stream velocity.	Limiting expanding check algorithm Area integration algorithm
Correct for surrounding momentum	Equivalent free stream velocity.	Corrected centreline velocity deficit	Equation 6.21 if applicable.
Evaluate the wake width	Corrected centreline deficit Position in optimisation loop	Domain on which to set-up the near wake model defined Wake width evaluated	Matrix set-up algorithm Equation 6.19
Evaluate the velocity deficit Gaussian profile	Corrected centreline deficit Model domain Wake width Elliptical wake widths (if available)	Near wake form	Gaussian equations

8 VALIDATION

8.1 Existing verification and validation GH near wake model

The authors were previously involved in an experimental testing programme of tidal turbines (TSB, 2006). These initial results show that the fundamental assumption that a Gaussian distribution represents the beginning of the far wake region is valid, although the exact relationship (velocity deficit as a function of ambient turbulence intensity and operating Ct) requires further experimental and full scale data, especially in more representative tidal flow conditions i.e. – higher turbulence intensity.

The figures below show that the fundamental properties of a tidal turbine wake are similar to a wind turbine wake, such that the wake develops into a Gaussian profile at the point where the shear layers meet the wake centreline. Although in these particular experiments the shear layers meet the centreline at around five diameters downstream (5D), the reasoning behind this is thought to be because of the very low ambient turbulence intensity in the flow.

Figure 8.2 shows the vertical and lateral velocity deficit profiles along with a contour plot at the 5D location. The axisymmetric Gaussian profile model yields very similar results to the experimental data providing confidence in the model. However further experimental work is required in order to build robust model that is checked at much higher ambient turbulence intensities, such that the location of the beginning of the far wake can be clearly identified. This is a primary objective of the experimental work packages included in PerAWaT. Further discussion on the PerAWaT validation requirements is given in the following section.

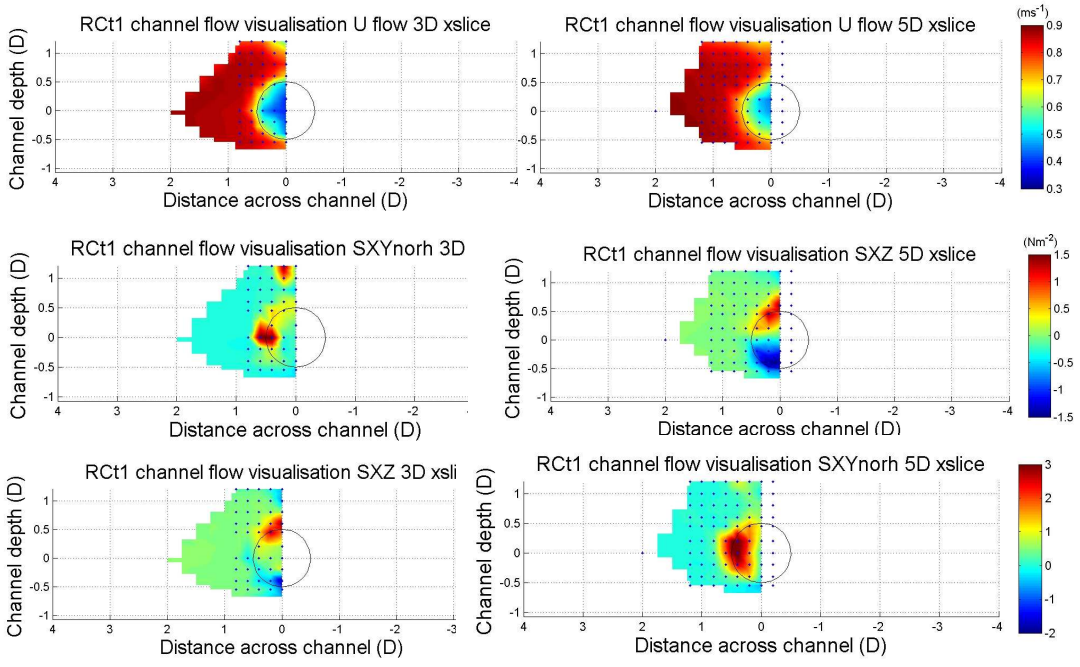

Figure 8-1 Wake form behind a 1/20th scale rotor operating in a large flume: top – velocity profile, middle lateral shear (Reynolds Stress), bottom - vertical shear (Reynolds Stress)

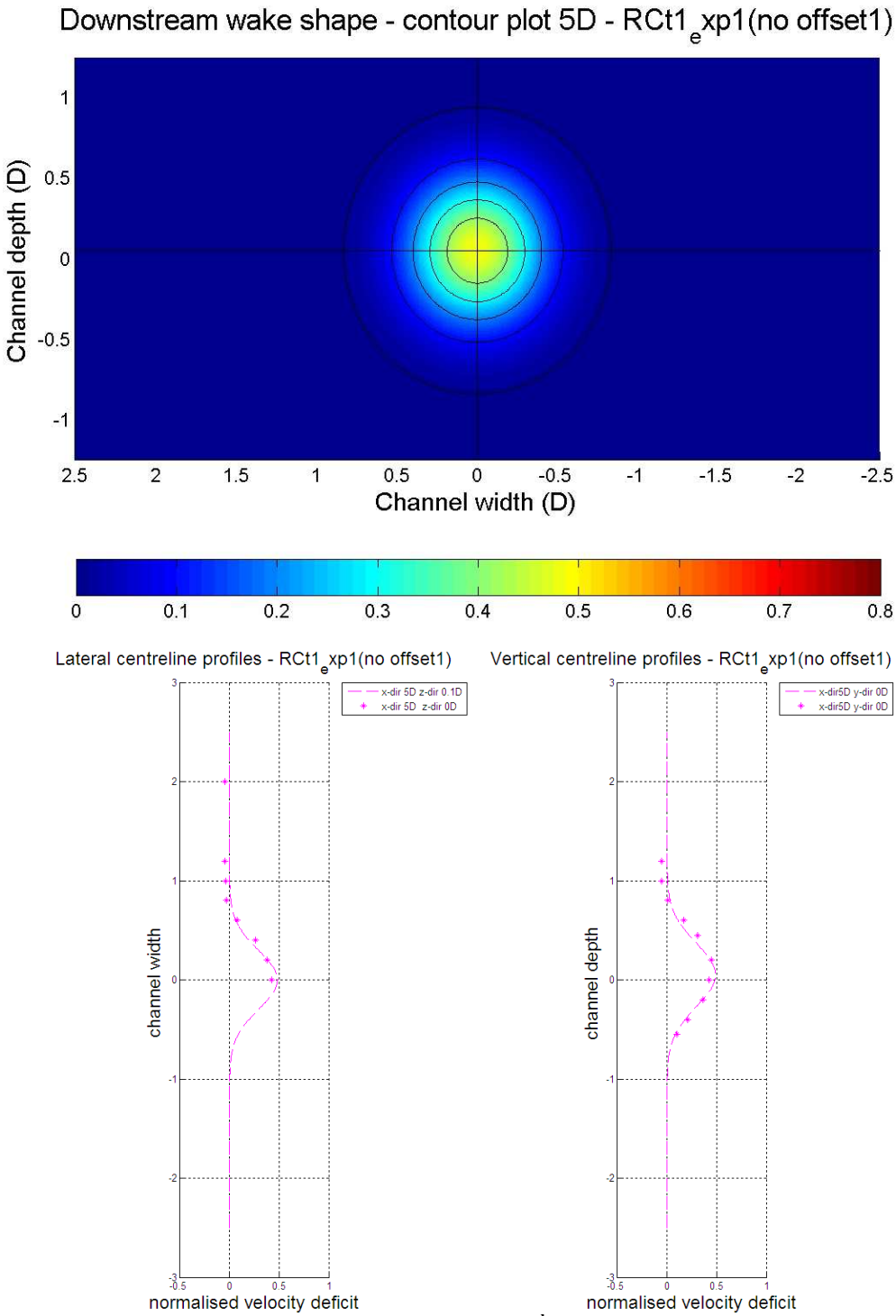

Figure 8-2 Comparison of the wake form behind a 1/20th scale rotor operating in a large flume and GH near wake prediction of the near wake form: left - 2-d fit of the experimental data, right – prediction vs measurement at 5D downstream.

8.2 Developments under PerAWaT

There are several key aspects of investigation in to near wake modelling within the PerAWaT project. Evaluating the flow field in and round the near wake region will be undertaken is a number of work packages via both experimental and numerical investigations. This will provided a large dataset for the development/validation of robust parametric models which look to capture the dominate factors affecting far wake modelling.

Experimentally the work packages WG4WP1, WG4WP2 & WG4WP3 all provide measured flow field maps of the near wake region. WG4WP1 provides single device scale measurements which look to better represent the complex nature of the near wake. WG4WP2 will provide multiple wake maps to provide indications of the effects of adjacent turbines. WG4WP3 will provide device scale wake maps behind open centre and duct turbines, allowing the applicability of the proposed near wake model to be investigated

Rotor performance and loading data from the ReDAPT (Reliable Data Acquisition Platform for Tidal) project will also be utilised if available. This data will further validate the application of this model for full scale scenarios.

The PerAWaT work packages WG3WP1& WG3WP5 will provide detail CFD simulation results of the near wake region to further investigate the effects of bounding surfaces and provide additional insight on how the near wake form varies for all three FDC.

The wide variety of numerical and physical validation tests will provide a robust set of tests to which the GH near wake model can be compared. The GH near wake model will be set up to be directly analogous with each test allowing direct comparison and thus validation of the model. The input parameters for comparison rotor performance (incorporating blockage), ambient flow turbulence intensity and the proximity to boundaries and/or other turbine wakes. The output parameters for comparison will be a map of flow field in the wake region.

Identification of where the shear layer meets the centreline in representative flow conditions is a primary aim of the near wake modelling work. The experimental, numerical and full scale data will allow a robust dataset for this to be investigated. Similarly the near wake shape and the influence on boundary proximity will be investigated.

One of the main aims of the PerAWaT project is to investigate the appropriateness of using the adapted Ainslie model to represent the wake behind a tidal turbine. This work will establish the impact of the change in flow conditions and the bounding effect of a free surface.

The impact of uncertainty around experimental and numerical results will be investigated to assess the impact on the near wake model uncertainty.

9 SUMMARY

This report describes the GH near wake model, including a literature review of the different modelling techniques. The theory and methodology of the GH near wake model have been detailed and an account of how the model will be incorporated in the Beta code is provided.

The GH near wake model is a semi-empirical model which will be extended to incorporate different ambient flow conditions via a variety of means:
- The empirical equations will be adjusted according to comparison with the results of other work package planned for PerAWaT (including the numerical work packages WG3WP1& WG3WP5 and the experimental work packages WG4WP1, WG4WP2 & WG4WP3).
- The effect of blockage will be incorporated by linking the model to the GH blockage model.

The next steps for this work package are:

- to analysis the experimental results provided from WG4WP1, WG4WP2 & WG4WP3;
- compare the results to the existing model and adjust as required;
- further compare the adjusted model with the numerical modelling results provided from WG3WP1& WG3WP5; and
- analysis and report on the uncertainty associated with the model in WG3WP4 D12.

10 BIBLIOGRAPHY

Abramovich G., The theory of turbulent jets. MIT Press Cambridge, Massachusetts, USA, 1963.

Ainslie, J. F., "Calculating the flowfield in the wake of wind turbines", Journal of Wind Enginering and Industrial Aerodynamics, 27: 213-224, 1988.

Ainslie, J. F., "Development of an eddy viscosity model for wind turbine wakes", Central Electricity Research Laboratories, Leatherhead, Surry. , 7th BWEA Conference Proceedings, Oxford, 1985

Bahaj, A.S., Myers, L.E., Thomson, M.D. & Jorge, N., "Characterising the wake of horizontal axis marine current turbines", Proceedings of 7th European Wave and Tidal Energy Conference, Porto, Portugal, 2007.

Barthelmie, R., Larsen, G., Pryor, S., Jørgensen, H., Bergström, H, Schlez, W., Rados, K, Vølund, P., Nechelmann, S., Schpers, G., Hegberg, T. & Folkerts, L., "Efficient development of offshore windfarms (ENDOW), Final report to the European Commission: Executive Summary. Report number ERK6-1999-0001. Risø-R-1407 (EN). 2003.

Connell, J.R. & George R.L., "The wake of the MOD-OA wind turbine two rotor diameters downwind" 3rd Dec 1981. Report No. PNL-4210, Pacific Northwest laboratory Battello, USA 1982.

Crespo, A, Hernández, J., Fraga, E. & Andreu, C, "Experimental validation of the UPM computer code to calculate wind turbine wakes and comparison with other models", Journal of Wind Enginering and Industrial Aerodynamics, 27, 77-88, 1988.

Crespo, A, Chacón, L., Hernández, J., Manuel, F., & Grau, J., "UPMPARK: a parabolic 3D code to model wind farms", Proceeding of the European Wind Energy Conference, Thessaloniki, 454-459, 1994.

Crespo, A. and Hernández, J., "Turbulence characteristics in wind-turbine wakes", Journal of Wind Engineering and Industrial Aerodynamics, 61: 71-85, 1996.

Crespo, A. and Hernández, J. & Frandsen, S. "Survey of modeling methods for wind turbine wakes and wind farms", Journal of Wind Energy, 2: 1-24, 1999.

Gant, S. & Stallard, T., "Modelling a tidal turbine in unsteady flow", Proceedings of the 18th International Offshore and Polar Engineering Conference, Vancouver, BC, Canada, 2008.

Garrad Hassan and Partners Ltd. Development of a design tool for axial flow tidal stream devices. BERR document, URN No. 08/852, Contract No. T/06/00231/00/00, 2008.

GH WindFarmer - Theory Manual, version 4.1, Garrad Hassan and Partners Ltd, February 2010.

GH WindFarmer Validation Manual, Garrad Hassan and Partners Ltd, Bristol, UK, 2003.

Hassan, U., A wind tunnel investigation of the wake structure within small wind turbine farms. Garrad Hassan and Partners, ETSU WN 5113, United Kingdom, 1993.

Katic I, Høstrup J and Jensen N, "A simple model for cluster efficiency", Proceedings of the BWEA Conference, 1986.

Leishman, J., Principles of helicopter aerodynamics. Cambridge Aerospace Series, Second Edition. 2006.

Li, Y. & Calisal, S. M., "Preliminary results of a vortex method for stand-alone vertical axis marine current turbine". Proceedings of the International Conference on Offshore Mechanics and Arctic Engineering (OMAE2007-29708), 2007.

Lissaman, P.B.S., "Energy effectiveness of arrays of wind energy conversion systems", Technical report AV FR 7058, AeroVironment Inc., Pasadena, California, USA, 1977.

Lissaman, P.B.S., "Energy effectiveness of arbitrary arrays of wind turbines", Journal of Energy, 3(6): 323-328, 1979.

Magnusson, M., "Near-wake behaviour of wind turbines". Journal of Wind Engineering and Industrial Aerodynamics, 80: 147-167, 1999.

Medici, D. & Alfredsson, P.H., "Measurements on a wind turbine wake: 3D effects and bluff-body vortex shedding", Proceedings of the Science of Making Torque from the Wind, Delft, 2004.

Mikkelsen, R., Actuator Disc Methods Applied to Wind Turbines. PhD Thesis, Department of Mechanical Engineering, Technical University of Denmark. 2003.

Münch, C., Vonlanthen, M., Gomes, J., Luquet, R, Guinard, P. & Avellan, F., "Design and performance assessment of a tidal ducted turbine". Proceedings of 3rd IAHR International meeting of the workgroup on cavitation and dynamic problems in hydraulic machinery and systems, Czech Republic, 2009.

Myers, L.E., Bahaj, A.S., Rawlinson-Smith, R.I., Thomson, M.D., "The effect of boundary proximity upon the wake structure of horizontal axis marine current turbines", Proceedings of 27th International Conference on Offshore Mechanics and Arctic Engineering, Estoril, Portugal, 2008.

Quarton, D.C. & Ainslie, A., P.B.S., "Turbulence in wind turbine wakes", Wind Engineering, 14(1), 1990.

Sezer-Uzol, N., & Long, L., "3-d time-accurate CFD simulations of wind turbine rotor flow fields". 44th AIAA Aerospace Sciences Meeting and Exhibit, Reno, Nevada, Jan. 9-12, 2006

Sforza, P.M., Sheerin, P. & Smorto, M., "Three-dimensional wakes of simulated wind turbines", AIAA Journal, 19(9) 1101-1107, 1981.

Simoes, F.J., & Graham J.M.R., "Prediction of loading on a horizontal axis wind turbine using a free vortex wake model." Proceedings of the BWEA Conference, 1991.

Sørensen, J.N., Shen, W.Z., & Munduate, X., "Analysis of wake states by a full-field actuator disc model." Wind Energy 1:73-88, 1998.

Sørensen, J.N., VISCWIND viscous effects on wind turbine blades. ET-AFM 9902, Department of Fluid Mechanics, The Technical University of Denmark, 1999.

Smith, G., Schlez, W., Liddell, A., Neubert, A. & Peña, A., "Characterising Advanced wake model for very closely spaced turbines", Proceedings of European Wind Energy Conference, Athens, Greece, 2006.

Tennekes, H. & Lumley, J.L., A first course in turbulence. MIT Press Cambridge, Massachusetts, USA, 1972.

Thake, J., (IT Power), Development, installation and testing of a large-scale tidal current turbine. DTI document, URN No. 05/1698, Contract No. T/06/0021/00/REP, 2005.

Tindal, A., Garrad, A., Schepers, G., Bulder, B., Hutting, H. & Verheij, F., "Dynamic loads in wind farms", Proceedings of the European Community Wind Energy Conference, 1993.

Technology Strategy Board (GRANT REFERENCE NO. T/06/00241/00/00 (200018) PERFORMANCE CHARACTERISTICS AND OPTIMISATION OF MARINE CURRENT ENERGY CONVERTER ARRAYS), 2005.

Vermeulen, P.E.J., "An experimental analysis of wind turbine wakes", 3rd Proc. International Symposium on Wind Energy Systems, Lyngby, 431-450, 1980.

Vermeer, L.J., Sorensen, J.N. & Crespo, A., "Wind turbine wake aerodynamics", Progress in Aerospace Sciences 39: 467-510, 2003.

Wang, T. & Coton, F., "Numerical simulation of wind tunnel wall effects on wind turbine flows". Wind Energy 3, 385-400. 2000.

Whelan, J. I., Graham, J. M. R., & Peiró, J., "A free-surface and blockage correction for tidal turbines". Journal of Fluid Mechanics 624, 281-291. 2009.

Zahle, F., Sorensen, N., Johnson, J., & Graham, J. Wind turbine rotor-tower interaction using an incompressible overset grid method. 45th AIAA Aerospace Sciences Meeting and Exhibit, Reno, Nevada, Jan. 8-11, 2007.

APPENDIX A GAUSSIAN DISTRIBUTION

Derivation of the relationship between velocity centerline deficit and the wake width.

A particular example of a 2D Gaussian function is

$$f(x,y) = Ae^{-\left(\frac{(x-x_o)^2}{2\sigma_x^2}\right)-\left(\frac{(y-y_o)^2}{2\sigma_y^2}\right)}.$$

Converting into polar coordinates and assuming zero offset i.e x_0 & y_0 and an axis-symmetric profile, then:

$$f(r) = A.e^{-\left(\frac{r^2}{2\sigma^2}\right)}$$

Note σ is the variance of the distribution if A(0) = 1/(2π σ^2). Comparing with Ainslie's model:

$$1-\frac{u(r)}{U_i} = D_m e^{-EM.\left(\frac{r}{B_w}\right)^2}$$

Then

$$A = D_m$$

And

$$2\sigma^2 = \frac{B_w^{\ 2}}{EM}$$

Where

$$u(r) = U_i\left(1-D_m e^{-EM.\left(\frac{r}{B_w}\right)^2}\right)$$

Substituting into the equation above and integrating over theta:

$$2\pi \int_0^\infty U_i^2 \left(1 - D_m e^{-EM.\left(\frac{r}{B_w}\right)^2} - \left(1 - D_m e^{-EM.\left(\frac{r}{B_w}\right)^2} \right)^2 \right) r dr = \frac{1}{2} C_t S U_i^2$$

$$2\pi \int_0^\infty U_i^2 \left(D_m e^{-EM.\left(\frac{r}{B_w}\right)^2} - D_m{}^2 e^{-2EM.\left(\frac{r}{B_w}\right)^2} \right) r dr = \frac{1}{2} C_t S U_i^2$$

Let $a^2 = \frac{B_W{}^2}{EM}$ and $b^2 = \frac{B_W{}^2}{2EM}$, then

$$2\pi \int_0^\infty D_m r e^{-\frac{r^2}{a^2}} - D_m{}^2 r e^{-\frac{r^2}{b^2}} dr = \frac{1}{2} C_t S$$

Using the integral

$$\int_0^\infty r^{2n+1} e^{-\frac{r^2}{a^2}} dr = \frac{n!}{2} a^{2n+1}$$

Then the equation above becomes:

$$2\pi \left(D_m \frac{a^2}{2} - D_m{}^2 \frac{b^2}{2} \right) = \frac{1}{2} C_t S$$

Where *S* is the rotor area in diameters ($S = \frac{\pi}{4}$), thus

$$\pi \frac{B_W{}^2}{EM} \left(D_m \left(1 - \frac{D_m}{2} \right) \right) = C_t \frac{\pi}{8}$$

$$B_W = \sqrt{\frac{EMC_t}{8D_m(1 - 0.5D_m)}}$$

where is found assuming that the wake width (B_w) used is defined as 1.89 times the half-width of the Gaussian profile.

APPENDIX B ELLIPTICAL GAUSSIAN PROFILE

A particular example of a 2D Gaussian function is

The general expression for a non axis-symmetric two-dimensional Gaussian function is:

$$f(x,y) = A\exp\left(-\left(a(x-x_o)^2 + b(x-x_o)(y-y_o) + c(y-y_o)^2\right)\right)$$

where

$$a = \left(\frac{\cos\theta}{\sigma_x}\right)^2 + \left(\frac{\sin\theta}{\sigma_y}\right)^2$$

$$b = -\frac{\sin 2\theta}{\sigma_x^2} + \frac{\sin 2\theta}{\sigma_y^2}$$

$$c = \left(\frac{\sin\theta}{\sigma_x}\right)^2 + \left(\frac{\cos\theta}{\sigma_y}\right)^2$$

As before the momentum deficit is:

$$\rho \int_A U_i^2 . \frac{u(r)}{U_i} - u(r)^2 dA = \frac{1}{2}\rho C_t S U_i^2$$

Where

$u(r) = U_i\left(1 - D_m e^{-EM.\left(\frac{r}{B_w}\right)^2}\right)$ becomes $u(z,y) = U_i\left(1 - D_m e^{-\frac{z^2}{2\sigma_z^2} - \frac{y^2}{2\sigma_y^2}}\right)$

So…

$$\rho \int_{-\infty}^{\infty}\int_{-\infty}^{\infty} U_i^2 \left(D_m e^{-\frac{z^2}{2\sigma_z^2}-\frac{y^2}{2\sigma_y^2}} - D_m^2 e^{-2\left(\frac{z^2}{2\sigma_z^2}-\frac{y^2}{2\sigma_y^2}\right)} \right) dzdy = \frac{1}{2}\rho C_t S U_i^2$$

$$\rho \int_{-\infty}^{\infty}\int_{-\infty}^{\infty} U_i^2 \left(D_m e^{-\frac{z^2}{2\sigma_z^2}-\frac{y^2}{2\sigma_y^2}} - D_m^2 e^{-2\left(\frac{z^2}{2\sigma_z^2}-\frac{y^2}{2\sigma_y^2}\right)} \right) dzdy = \frac{1}{2}\rho C_t S U_i^2$$

Using the integral

$$\int_{-\infty}^{\infty} ae^{-(x+b)^2/c^2}\,dx. \quad = a|c|\sqrt{\pi}.$$

then

$$2\pi\sigma_z\sigma_y\left(D_m - \frac{D_m^2}{2}\right) = \frac{1}{2}C_t S$$

Where *S* is the rotor area in diameters ($S = \frac{\pi}{4}$), thus

$$2\pi\sigma_z\sigma_y\left(D_m\left(1-\frac{D_m}{2}\right)\right) = C_t\frac{\pi}{8}$$

Using $\sigma_z^2 = \frac{B_z^2}{2EM}$, then

$$B_z B_y = \sqrt{\frac{EMC_t}{8D_m(1-0.5D_m)}}$$

And the momentum deficit can be evaluated from

$$2\pi\sigma_z\sigma_y\left(D_m - \frac{D_m^2}{2}\right)\rho U_i^2$$